Supplementary Information for

Loss of insulin signaling contributes to atrial fibrillation and atrial electrical remodeling in type I diabetes mellitus

Iuliia Polina, Hailey J. Jansen, Tiesong Li, Motahareh Moghtadaei, Loryn J. Bohne, Yingjie Liu, Pooja Krishnaswamy, Emmanuel E. Egom, Darrell D. Belke, Sara A. Rafferty, Martin Ezeani, Anne M. Gillis, Robert A. Rose

Robert Rose
robert.rose@ucalgary.ca

Supplemental Methods

Mice

Male littermate wildtype and type 1 diabetic Akita mice (1, 2) between the ages of 16 and 22 weeks were used in this study. At this age range, hyperglycemia has developed to a stable level (2, 3). Akita mice were initially obtained from the Jackson Laboratory (strain C57BL/6-*Ins2*^{Akita}/J) and then bred locally. This mouse contains a mutation in the insulin-2 (*Ins2*) gene, *Ins2*^{C96Y}, which results in severe pancreatic β cell dysfunction and development of the diabetic phenotype (4). Heterozygous Akita mice (diabetic) and littermate wildtypes were used in this study. The diabetic phenotype was determined by assessing urine glucose (using keto-diastix reagent strips for urinalysis) as well as serum glucose levels (using a glucometer).

In some experiments, male wildtype C57BL/6 mice were treated with streptozotocin (STZ) to induce Type 1 DM (4). For these studies, mice were fasted for 6 hrs and then given an injection of STZ (50 mg/kg; intraperitoneal), or vehicle control (citrate buffer), once a day for 5 consecutive days (5). STZ injected mice developed hyperglycemia and were used experimentally 6 weeks after STZ injections were completed. Mice were 16-18 weeks of age at the time of experimental use.

In some cases Akita mice were treated with chronically with insulin (or placebo) for 4 weeks beginning at 12 weeks of age. This was done by implanting insulin or placebo pellets

(LinShin Canada) subcutaneously (2). These pellets release 0.2 units of insulin/day. Mice were anesthetized by isoflurane inhalation (3%) and pellets were implanted via a small puncture in the skin according to the manufacturer's instructions. Blood glucose was monitored in these animals before pellet implantation and then every 3 days after treatment began until the animals were used experimentally at 16 weeks of age. In other studies Akita mice were given acute intraperitoneal injections of insulin (5-10 U/kg), or saline as a control. 30-45 min later blood glucose was measured to ensure it was reduced and then the mice with used experimentally. In experiments in which atrial myocytes were isolated from mice acutely injected with insulin, these cells were used experimentally within 2 hours of isolation.

In vivo electrophysiology

Mice were anesthetized by isoflurane inhalation and subdermal needle electrodes (30 gauge) were placed around the heart in a lead II conformation. Surface ECG recordings were used to measure standard ECG parameters including RR interval, P wave duration, and PR interval.

A 1.2 French octapolar electrophysiology catheter containing 8 electrodes spaced 0.5 mm apart was used for intracardiac pacing experiments as we have described previously (6, 7). Inducibility of AF was studied using burst pacing in the right atrium (6, 7). We used 3 trains of 2 s burst pacing as follows: the first 2 s burst was given at a cycle length of 40 ms with a pulse duration of 5 ms. Following 3 min of stabilization a second 2 s burst was applied at a cycle length 20 ms with a pulse duration of 5 ms. After another 3 min of stabilization the final 2 s burst was given at a cycle length of 20 ms with a pulse duration of 10 ms. AF was defined as a rapid and irregular atrial rhythm (fibrillatory baseline in the ECG) with irregular RR intervals lasting at least 1 s on the surface ECG and the intracardiac atrial electrogram during any of the burst pacing protocols. All ECG data were acquired using a Gould ACQ-7700 amplifier and Ponemah

Physiology Platform software (Data Sciences International) as we have described previously (6, 7).

High resolution optical mapping

To study patterns of electrical conduction in the mouse atria we used high resolution optical mapping in atrial preparations as we (8) and others (9, 10) have done previously. To isolate our atrial preparation mice were administered a 0.2 ml intraperitoneal injection of heparin (1000 IU/ml) to prevent blood clotting and were then anesthetized by isoflurane inhalation and cervically dislocated. Hearts were excised into Krebs solution (35°C) containing (in mM): 118 NaCl, 4.7 KCl, 1.2 KH_2PO_4, 12.2 $MgSO_4$, 1 $CaCl_2$, 25 $NaHCO_3$, 11 glucose and bubbled with 95% O_2/5% CO_2 in order to maintain a pH of 7.4. The atria were dissected away from the ventricles and pinned in a dish with the epicardial surface facing upwards (towards the imaging equipment). The superior and inferior vena cavae were cut open so that the crista terminalis could be visualized and the preparation could be pinned out flat.

The atrial preparation was superfused continuously with Krebs solution (35°C) bubbled with 95% O_2/5% CO_2 and allowed to equilibrate for at least 30 min before data collection ensued. During this time the preparation was treated with the voltage sensitive dye di-4-ANEPPS (10 µM) for ~15 min and blebbistatin (10 µM) was added to the superfusate to suppress contractile activity (11, 12). Blebbistatin was present throughout the duration of the experiments in order prevent motion artifacts during optical mapping. Optical mapping studies were conducted on atrial preparation in sinus rhythm.

Di-4-ANEPPS loaded atrial preparations were illuminated with light at a wavelength of 520 – 570 nM using an EXFO X-cite fluorescent light source (Lumen Dynamics). Emitted light (590 – 640 nM) was captured using a high speed EMCCD camera (Evolve 128, Photometrics). Data were captured from an optical field of view of 8 x 8 mm^2 at a frame rate of ~900 frames/s

using Metamorph software (Molecular Devices). The spatial resolution was 67 x 67 µM for each pixel. Magnification was constant in all experiments and no pixel binning was used.

All optical data were analyzed using custom software written in Matlab. Pseudocolor electrical activation maps were generated from measurements of activation time at individual pixels as defined by assessment of dF/dt_{max}. In all cases background fluorescence was subtracted. Local conduction velocity (CV) was quantified specifically in the right atrial myocardium (within the RAA) and the left atrial myocardium (within the LAA) using an established approach previously described (8, 9, 13). Briefly, activation times at each pixel from a 7 x 7 pixel array were determined and fit to a plane using the least squares fit method. The direction on this plane that is increasing the fastest represents the direction that is perpendicular to the wavefront of electrical propagation and the maximum slope represents the inverse of the speed of conduction in that direction. With a spatial resolution of 67 x 67 µM per pixel, the area of the 7 x 7 pixel array was 469 x 469 µM. Five CV measurements were made in each region and averaged. Thus, using this method, we computed maximum local CV vectors in the atrial region of interest.

Isolation of mouse atrial myocytes

The procedures for isolating mouse atrial myocytes have been described previously (14, 15) and were as follows. Mice were administered a 0.2 ml intraperitoneal injection of heparin (1000 IU/ml) to prevent blood clotting. Following this, mice were anesthetized by isoflurane inhalation and then sacrificed by cervical dislocation. The heart was excised into Tyrode's solution (35ºC) consisting of (in mM) 140 NaCl, 5.4 KCl, 1.2 KH_2PO_4, 1.0 $MgCl_2$, 1.8 $CaCl_2$, 5.55 glucose, and 5 HEPES, with pH adjusted to 7.4 with NaOH. The right or left atrial appendage was dissected from the heart and cut into strips, which were transferred and rinsed in a 'low Ca^{2+}, Mg^{2+} free' solution containing (in mM) 140 NaCl, 5.4 KCl, 1.2 KH_2PO_4, 0.2 $CaCl_2$, 50 taurine, 18.5 glucose, 5 HEPES and 1 mg/ml bovine serum albumin (BSA), with pH adjusted to

6.9 with NaOH. Atrial tissue was digested in 5 ml of 'low Ca^{2+}, Mg^{2+} free' solution containing collagenase (type II, Worthington Biochemical Corporation), elastase (Worthington Biochemical Corporation) and protease (type XIV, Sigma Chemical Company) for 30 min. Then the tissue was transferred to 5 ml of modified KB solution containing (in mM) 100 potassium glutamate, 10 potassium aspartate, 25 KCl, 10 KH_2PO_4, 2 $MgSO_4$, 20 taurine, 5 creatine, 0.5 EGTA, 20 glucose, 5 HEPES, and 0.1% BSA, with pH adjusted to 7.2 with KOH. The tissue was mechanically agitated using a wide-bore pipette. This procedure yielded individual right or left atrial myocytes that were stored in KB solution until experimental use within 6 hours of isolation. Identical isolation procedures were used for wildtype and Akita mice and there were no discernable differences in cell yield or cell quality between groups during patch-clamp experiments.

Isolation of mouse ventricular myocytes

Mice were anesthetized by isoflurane inhalation and then euthanized by cervical dislocation. The heart was excised and retrogradely perfused with myocyte buffer (35°C) consisting of (in mM) 113 NaCl, 4.7 KCl, 1.2 $MgCl_2$, 0.6 KH_2PO_4, 0.6 NaH_2PO_4, 5 BDM (2,3-butanedione monoximine), 1.6 $NaHCO_3$, 30 taurine, 20 glucose, and 10 HEPES, with pH adjusted to 7.4 with NaOH. After the initial 2-3 minutes, the myocyte buffer was switched to digestion solution containing 0.1 mM $CaCl_2$, collagenase (type II, Worthington Biochemical Corporation) and protease (type XIV, Sigma Chemical Company) and the heart was perfused for 10-12 minutes at a flow rate of 1 ml/min. Finally, the heart was perfused with stopping buffer (myocyte buffer containing 2.5% bovine serum albumin and 0.1 mM $CaCl_2$) for another 2-3 minutes. After perfusion, the ventricles were excised and transferred to 5 ml of stopping buffer. The tissue was mechanically disaggregated using forceps and gently triturated with a 10 ml serological pipette. Then another 5 ml of fresh stopping buffer was added to bring the volume to

10 ml. $CaCl_2$ ws added to restore the Ca^{2+} concentration to 0.5 mM in four steps every 5 minutes.

Solutions and electrophysiological protocols

Stimulated action potentials (APs) were recorded using either the perforated patch-clamp technique or the whole cell patch-clamp technique. The latter was used to allow compounds to be dialyzed into cells via the patch pipette. There were no differences in AP parameters between perforated and whole cell configurations. To record APs the recording chamber was superfused with a normal Tyrode's solution (22 – 23ºC) containing (in mM) 140 NaCl, 5 KCl, 1 $MgCl_2$, 1 $CaCl_2$, 10 HEPES, and 5 glucose, with pH adjusted to 7.4 with NaOH. The pipette filling solution contained (in mM) 135 KCl, 0.1 $CaCl_2$, 1 $MgCl_2$, 5 NaCl, 10 EGTA, 4 Mg-ATP, 6.6 Na-phosphocreatine, 0.3 Na-GTP and 10 HEPES, with pH adjusted to 7.2 with KOH. Amphotericin B (200 µg/ml) was added to this pipette solution to record APs with the perforated patch clamp technique. APs were stimulated with a 20 ms depolarizing pulses of 0.6-0.7 nA.

For recording I_{Na} atrial myocytes were superfused with a modified Tyrode's solution (22 – 23°C) containing the following (in mM): 130 CsCl, 5 NaCl, 5.4 TEA-Cl, 1 $MgCl_2$, 1 $CaCl_2$, 10 HEPES, 5.5 glucose, (pH 7.4, adjusted with CsOH). Nitrendipine (10 µM) was added to the superfusate to block $I_{Ca,L}$. The pipette solution for I_{Na} contained (in mM): 120 CsCl, 5 NaCl, 1 $MgCl_2$, 0.2 $CaCl_2$, 10 HEPES, 5 MgATP, 0.3 Na-GTP, 5 BAPTA (pH 7.2, adjusted with CsOH). I_{Na} was recorded using 50 ms voltage clamp steps between -100 and 10 mV from a holding potential of -120 mV. I_{Na} activation kinetics were determined by calculating chord conductance (G) with the equation $G=I/(V_m-E_{rev})$, where V_m represents the depolarizing voltages and E_{rev} is the reversal potential estimated from the current-voltage relationships of $I_{Ca,L}$ or I_{Na}. Maximum conductance (G_{max}) and $V_{1/2}$ of activation for $I_{Ca,L}$ and I_{Na} were determined using the following function: $G=[(V_m-V_{rev})][G_{max}][-1/[(1+\exp((V_m-V_{1/2})/k))+1]]$. I_{Na} inactivation kinetics were measured

using 500 ms pre-pulse voltage clamp steps between -120 and -30 mV from a holding potential of -120 mV followed by a 20 ms test pulse to -20 mV. Normalized peak currents were plotted as a function of the pre-pulse potential and the resulting curve was fitted with the Boltzmann function $h=1/[1+\exp[V_{1/2}-V]/k]$. These data were used to measure the voltage at which 50% of channels are inactivated ($V_{1/2(act)}$).

Potassium currents (I_K) were recorded in the whole cell configuration using the normal Tyrode's solution and pipette solution as used to record APs. To record total potassium currents (no pre-pulse), cells were held at -80 mV then I_K was recorded using voltage clamp steps (500 ms duration) between -120 and +80 mV in 10 mV increments. To record potassium currents with an inactivating pre-pulse (to inactivate I_{to}), cells were given a 200 ms pre-pulse to -40 mV immediately followed by 500 ms voltage clamp steps from -120 to +80 mV from a holding potential of -80 mV. For these recordings with and without a pre-pulse recordings, I_K was measured at the peak current for each voltage step. I_{to} was calculated as the difference current between the recording with and without a pre-pulse (16, 17).

I_{Kur}, as carried by Kv1.5 channels, was measured as the component of I_K sensitive to 4-aminopyradie (4-AP; 100 µM) (16, 18). The voltage clamp protocol for measuring I_{Kur} included a pre-pulse to -40 mV for 200 ms to inactivate I_{to} immediately followed by a 500 ms step to +30 mV before returning to a holding potential of -80 mV. Peak currents at baseline, in the presence of 4-AP, and after washout were measured.

For recording $I_{Ca,L}$ atrial myocytes were superfused with a modified Tyrode's solution (22 – 23ºC) containing the following (in mM) 145 TEA-Cl, 2 $CaCl_2$, 1 $MgCl_2$, 10 HEPES, and 5 glucose with pH adjusted to 7.4 with NaOH. The pipette solution for $I_{Ca,L}$ contained (in mM) 135 CsCl, 0.1 $CaCl_2$, 1 $MgCl_2$, 5 NaCl, 10 EGTA, 4 Mg-ATP, 6.6 Na-phosphocreatine, 0.3 Na-GTP and 10 HEPES, with pH adjusted to 7.2 with CsOH. $I_{Ca,L}$ was recorded from a holding potential of -60 mV due to the expression of $Ca_V1.2$ and $Ca_V1.3$ in atrial myocytes (14, 15, 19, 20). Thus,

our voltage clamp protocols enable us to record total $I_{Ca,L}$, which could include contributions from $Ca_V1.2$ as well as $Ca_V1.3$.

For recording $I_{Na,L}$ atrial myocytes were superfused with a modified Tyrode's solution (22-23 ºC) containing the following (in mM): 135 NaCl, 5 TEA-Cl, 4 CsCl, 2 $MgCl_2$, 10 glucose, 10 HEPES, 0.03 niflumic acid, 0.004 strophanthidin, and 0.01 nifedipine with pH adjusted to 7.4 with NaOH. The pipette solution for $I_{Na,L}$ contained (in mM) 130 CsCl, 5 NaCl, 1 $MgCl_2$, 0.2 $CaCl_2$, 10 HEPES, 5 Mg-ATP, 0.3 Na-GTP, 10 EGTA with pH adjusted to 7.2 with CsOH. $I_{Na,L}$ was recorded using 1 s voltage clamp steps to -35 mV from a holding potential of -120 mV. $I_{Na,L}$ was measured as an integral from 100-150 ms after peak I_{Na}.

To study early afterdepolarization (EAD) susceptibility, APs were recorded at pacing frequencies of 2, 1, 0.2 and 0.1 Hz in baseline conditions and in the presence of 1 μM isoproterenol (ISO). A minimum of 30 APs were recorded in each condition and at each pacing frequency and examined for the occurrence of EADs.

Micropipettes were pulled from borosilicate glass (with filament, 1.5 mm OD, 0.75 mm ID, Sutter Instrument Company) using a Flaming/Brown pipette puller (model p-87, Sutter Instrument Company). The resistance of these pipettes was 4 – 8 MΩ when filled with recording solution. Micropipettes were positioned with a micromanipulator (Burleigh PCS-5000 system) mounted on the stage of an inverted microscope (Olympus IX71). Seal resistance was 2 – 15 GΩ. Rupturing the sarcolemma in the patch for voltage clamp experiments resulted in access resistances of 5 – 15 MΩ. Series resistance compensation averaged 80 – 85% using an Axopatch 200B amplifier (Molecular Devices). Capacitative currents were not subtracted from currents. Recorded signals were filtered with a 1 KHz low pass Bessel filter. For perforated patch clamp experiments access resistance was monitored for the development of capacitative transients upon sealing to the cell membrane with Amphotericin B in the pipette. Typically, access resistance became less than 25 MΩ within 5 min of sealing onto the cell, which was sufficient for recording stimulated APs in current clamp mode. Data were digitized using a

Digidata 1440 and pCLAMP 10 software (Molecular Devices) and stored on computer for analysis.

Quantitative PCR

Total RNA was isolated from right or left atrial appendages using a PureZOL™ RNA Isolation Reagent and the Aurum™ Total RNA Fatty and Fibrous Tissue Kit (Bio-Rad Laboratories) as per kit instructions. RNA samples were eluted from the spin column in 40 µL elution buffer. RNA yield and purity were assessed using a Nanodrop. All samples had a A_{260}/A_{280} of over 2.0 and therefore were free of DNA contamination. Next, cDNA (20 ng/µL) was synthesized using the iScript™ cDNA Synthesis Kit (Bio-Rad Laboratories). Reactions were performed in a Bio-Rad MyCycler thermal cycler using the following protocol: 5 min of priming at 25ºC followed by reverse transcription for 30 min at 42ºC then 5 min at 85ºC to inactivate reverse transcriptase.

All qPCR reactions were run in duplicate in 10 µL reactions that contained the following: 4 µL sample cDNA, 5.6 µL GoTaq® qPCR Master Mix (Promega), and 0.4 µL primers. Primers were reconstituted to a final concentration of 100 µM with nuclease free water and stored at -20ºC until use. Primers were diluted to 10 µM for qPCR reactions. RT-qPCR reactions were performed using the CFX386 Touch™ Real-Time PCR Detection System (Bio-Rad) using the following protocol: Taq polymerase was activated for 2 min at 95ºC followed by 39 cycles of denaturing for 15 s at 95ºC, annealing for 30 s at 60ºC, and extension for 30s at 72ºC. This was followed by melt curve analysis from 65-95ºC in 0.5ºC increments. Data were analyzed using the $2^{-\Delta\Delta C}{}_T$ method using the CFX Manager Software version 3.1 (Bio-Rad). Gene expression was normalized to GAPDH. Primer sequences are listed in Supplemental Table 17 below.

Western blotting

Atria were homogenized in an ice-cold RIPA buffer (50 mM Tris, 150 mM NaCl, 1 mM EDTA, 0.5% sodium Deoxycholic, 1% NP-40, 0.1% SDS) containing 2mM phenylmethane sulfonyl fluoride (Sigma), Halt™ Protease Inhibitor Cocktail (Thermo Fisher scientific). Preparations were centrifuged at 15000 rpm for 30 mins. Protein concentrations were measured using a Bio-Rad *DC*™ Protein Assay Kit II (Bio-Rad Laboratories). Protein samples (30 µg/lane) were separated by 7.5% SDS-polyacrylamide gels (SDS-PAGE) and transferred onto Immun-Blot® PVDF membrane (Bio-Rad). The membrane was blocked with 5% milk in Tris-buffer saline Tween-20 (TBST) for 1 hour and then incubated overnight at 4^0C with primary antibodies (Kv1.5 1:500, Kv4.2 1:500, Kv4.3 1:500, Nav1.5 1:500, all from Alomone Labs or GAPDH 1:2000, Abcam). The membrane was washed with TBST and then incubated with goat anti-rabbit IgG coupled to horseradish peroxidase (HRP) at 1:4000 for 1 hour at room temperature. ECL (Bio-Rad) was added and membrane was scanned using the ChemiDoc XRS+ system (Bio-Rad).

Calcium transients

Calcium transients were measured using confocal imaging in acutely isolated atrial myocytes. Right atrial myocytes were loaded with 5 µg/ml Rhod-2-AM for 15 minutes in a chamber pre-coated with 50 µg/ml R-laminin. After dye loading the cell chamber was washed to remove any excess dye by superfusing the myocytes with KRH buffer (125 mM NaCl, 5 mM KCl, 1.2 mM $MgCl_2$, 1.2 mM KH_2PO_4, 25 mM HEPES and 12 mM glucose, pH=7.4) containing 1mM $CaCl_2$ and then switched to KRH containing 1.8mM $CaCl_2$ and 5µM (S)-(-)-Blebbistatin. The myocytes were field stimulated (24 V) using a stimulation chamber (Warner Instruments) at 1 Hz. Recordings were obtained at 37°C using a Nikon confocal microscope with NIS-Elements AR software by performing line scans longitudinally along the cell membrane. Calcium transient morphology was analyzed using Clampfit. Paramters analyzed include the time to peak (T_{peak}) and time to 25%, 50%, 75% and 90% decay (T_{25}, T_{50}, T_{75} and T_{90}).

Supplemental Figures

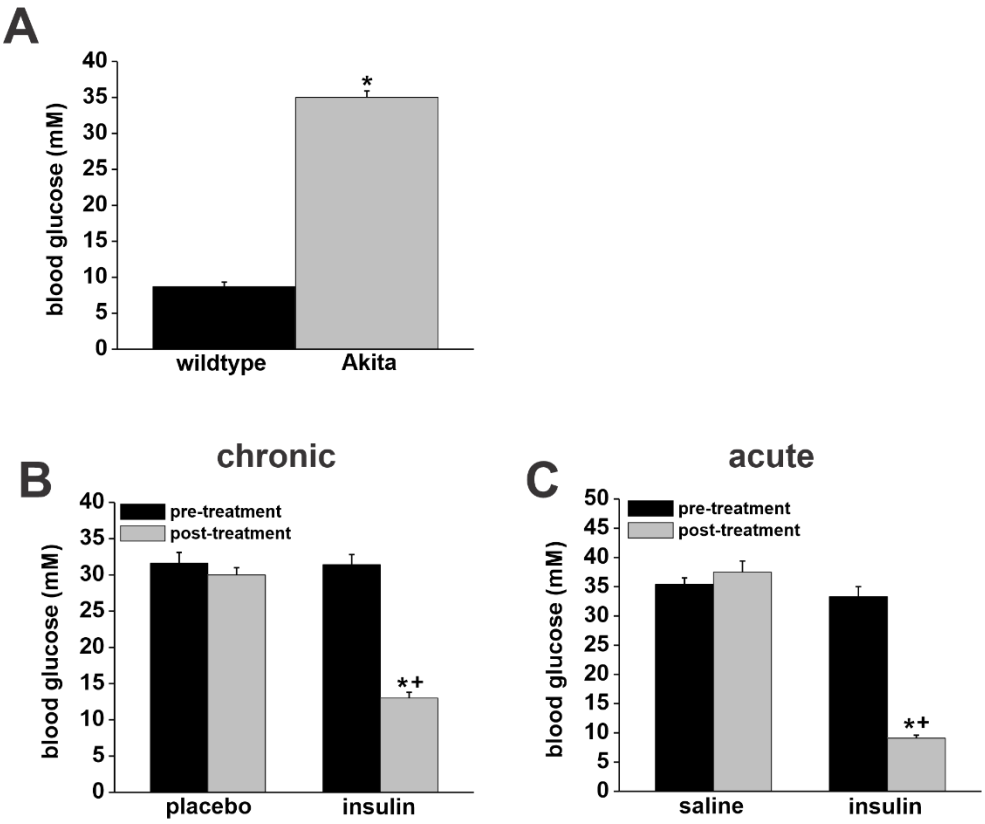

Figure S1. Blood glucose measurements. (*A*) Blood glucose values in wildtype and Akita mice. **P*<0.05 vs. wildtype by Student's *t*-test, *n*=22 wildtype and 27 Akita mice. (*B*) Blood glucose values in Akita mice at baseline (pre-treatment) and after 4 weeks of insulin treatment (post-treatment). **P*<0.05 vs. pre-treatment, ^{+}P<0.05 vs. saline by two-way ANOVA with Tukey's posthoc test, *n*=21 Akita mice for placebo and 24 for chronic insulin. (*C*) Blood glucose values in Akita mice at baseline (pre-treatment) and 30-45 min after injection with insulin (post-treatment). **P*<0.05 vs. pre-treatment, ^{+}P<0.05 vs. saline injection by two-way ANOVA with Tukey's posthoc test, *n*=11 Akita mice for saline and 16 for acute insulin.

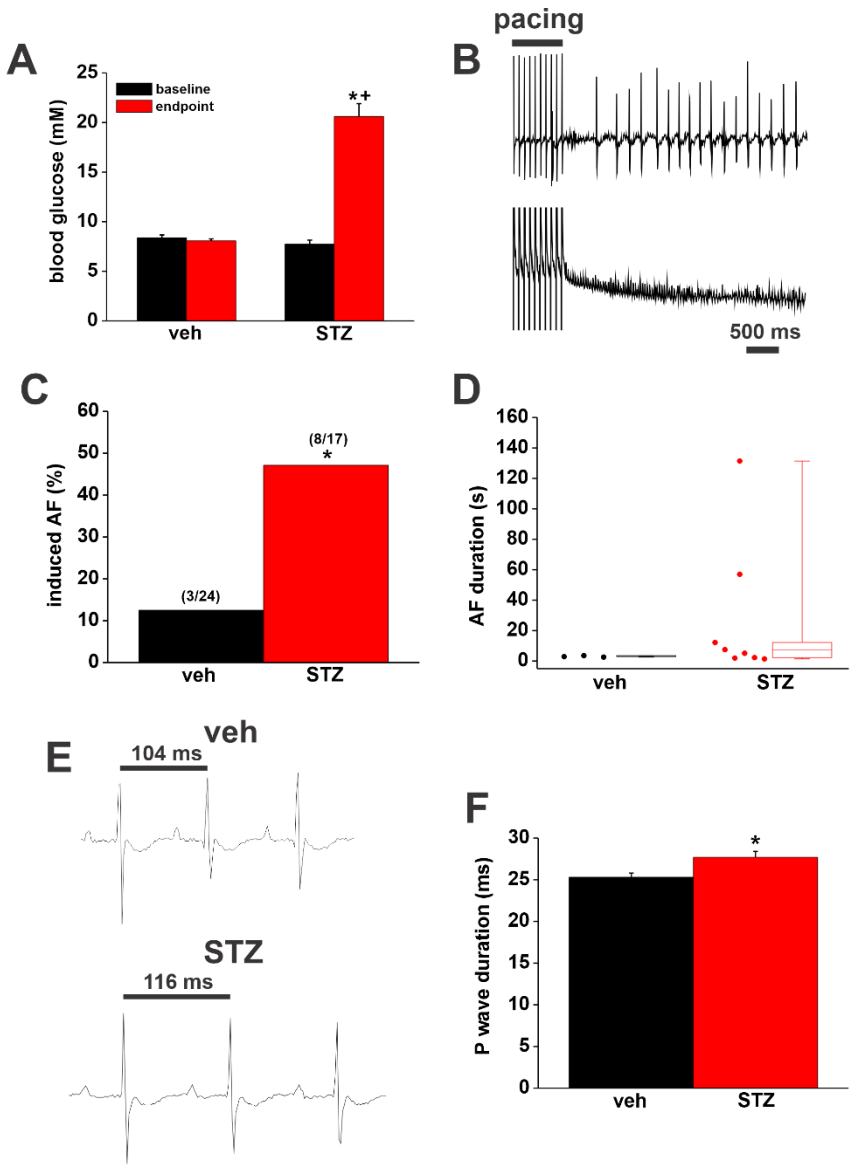

Figure S2. Atrial fibrillation and atrial electrophysiology in STZ injected diabetic mice. (*A*) blood glucose values at baseline and endpoint after STZ or vehicle (veh) injection. **P*<0.05 vs. baseline; $^{+}$*P*<0.05 vs. veh by two-way ANOVA with Tukey's posthoc test; *n*=24 veh and 17 STZ mice. (*B*) Representative surface (top) and intracardiac atrial (bottom) electrograms illustrating the induction of AF in an STZ treated mouse. (*C*) Susceptibility to induced AF in veh and STZ injected mice **P*<0.05 by Fischer's exact test. (*D*) Duration of AF in veh and STZ injected mice that were induced into AF. (*E*) Representative surface ECGs in veh and STZ injected mice. (*F*) Summary of P wave durations in veh and STZ injected mice. **P*<0.05 vs. veh by Student's *t*-test.

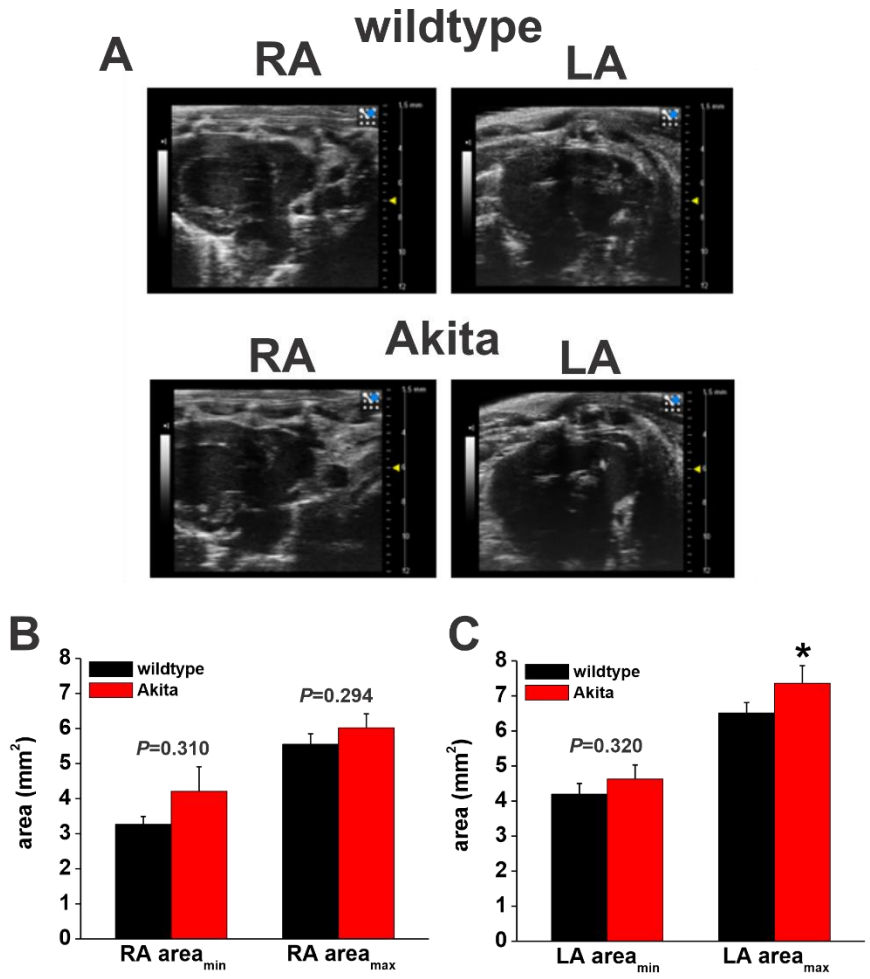

Figure S3. Echocardiography in Akita mice. (*A*) Representative images used to assess right atrial (RA) and left atrial (LA) area in wildtype and Akita mice. Bars on left side of images represent contrast intensity. Scale bars on right side of images are measures of distance (mm). (*B*) Minimum and maximum RA area in wildtype and Akita mice. (*C*) Minimum and maximum LA area in wildtype and Akita mice. **P*<0.05 vs. wildtype by two-way ANOVA with Tukey's posthoc test; *n*=11 mice per group. Refer to Table S9 for a summary of echocardiography analysis.

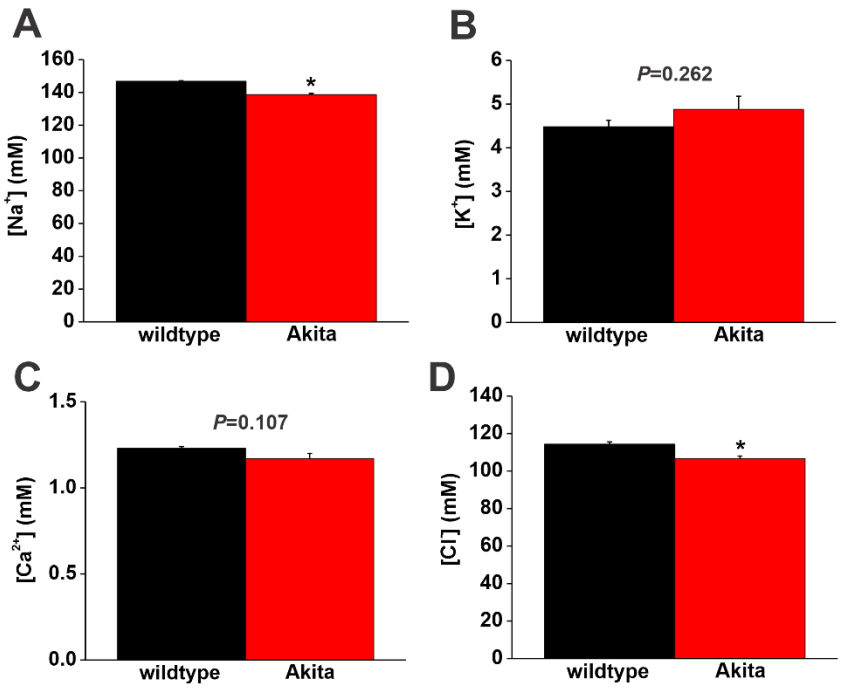

Figure S4. Blood electrolytes in Akita mice. Blood concentrations of Na^+ (*A*), K^+ (*B*), Ca^{2+} (*C*) and Cl^- (*D*) in wildtype and Akita mice. **P*<0.05 vs. wildtype by Student's *t*-test; *n*=6 mice per group.

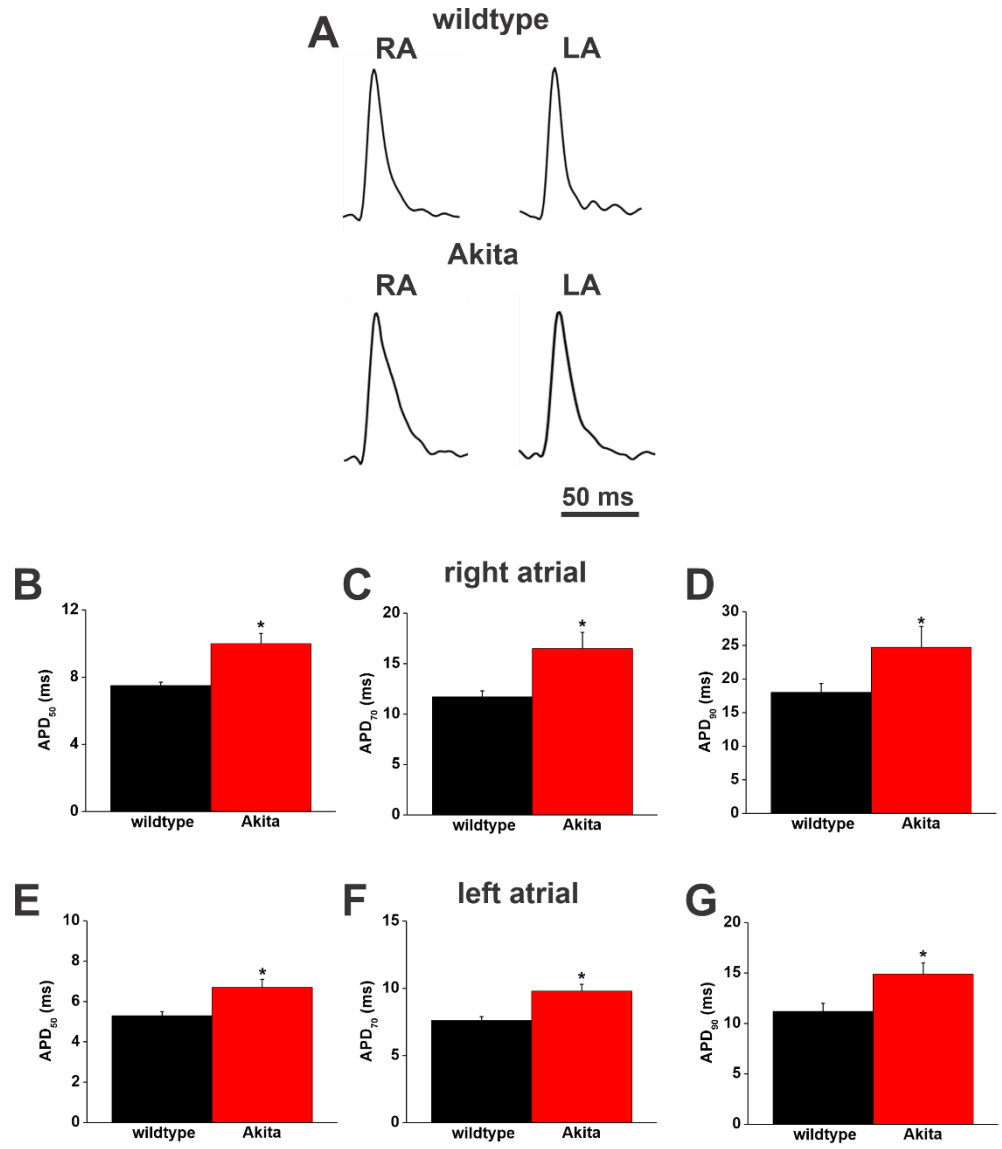

Figure S5: Optical action potential duration in wildtype and Akita mice. (*A*) Representative optical APs in right and left atria from wildtype and Akita mice. (*B-D*) Summary of right atrial APD_{50} (*B*), APD_{70} (*C*) and APD_{90} (*D*) for wildtype and Akita mice. (*E-G*) Summary of left atrial APD_{50} (*E*), APD_{70} (*F*), and APD_{90} (*G*). *$P<0.05$ vs. wildtype by Student's *t*-test; $n=5$ hearts per group.

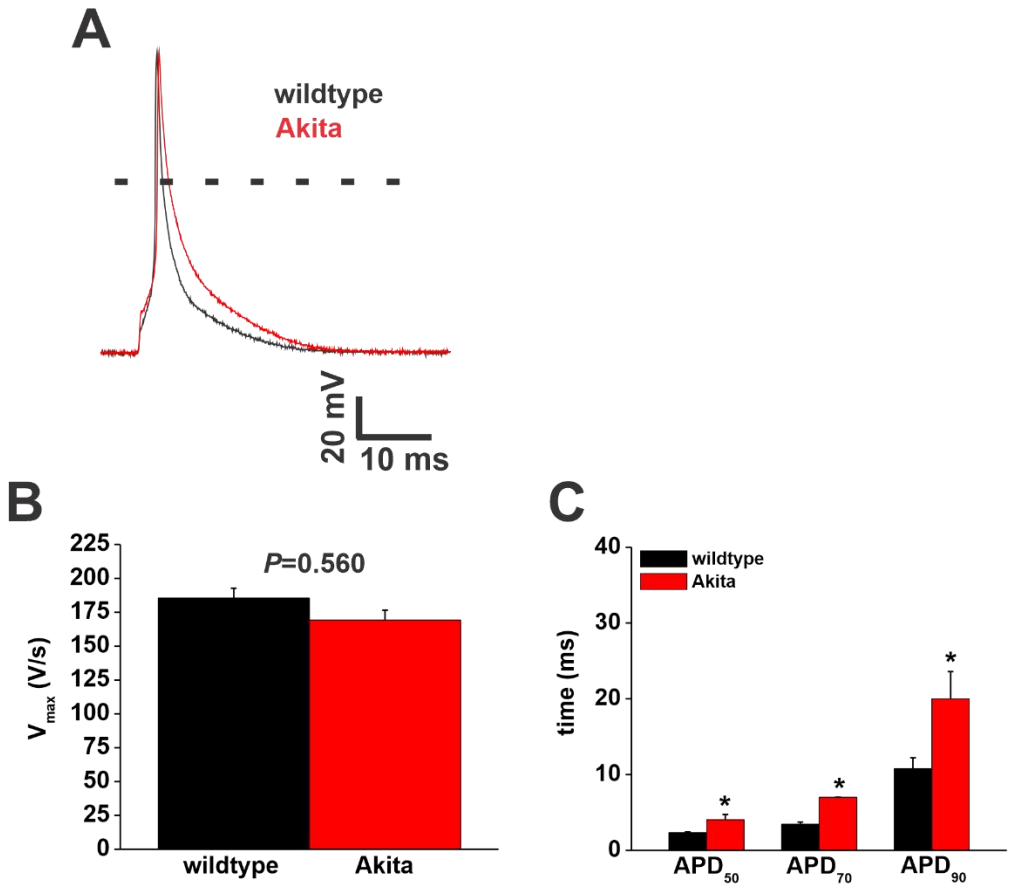

Figure S6: Ventricular myocyte action potential morphology in Akita mice. (*A*) Representative stimulated APs in isolated ventricular myocytes from wildtype and Akita mice. (*B*) AP V_{max} in isolated ventricular myocytes from wildtype and Akita mice. (*C*) AP duration at 50% (APD_{50}), 70% (APD_{70}) and 90% (APD_{90}) repolarization in wildtype and Akita mice. **P*<0.05 vs. wildtype by Student's *t*-test; *n*=8 for wildtype and 11 for Akita.

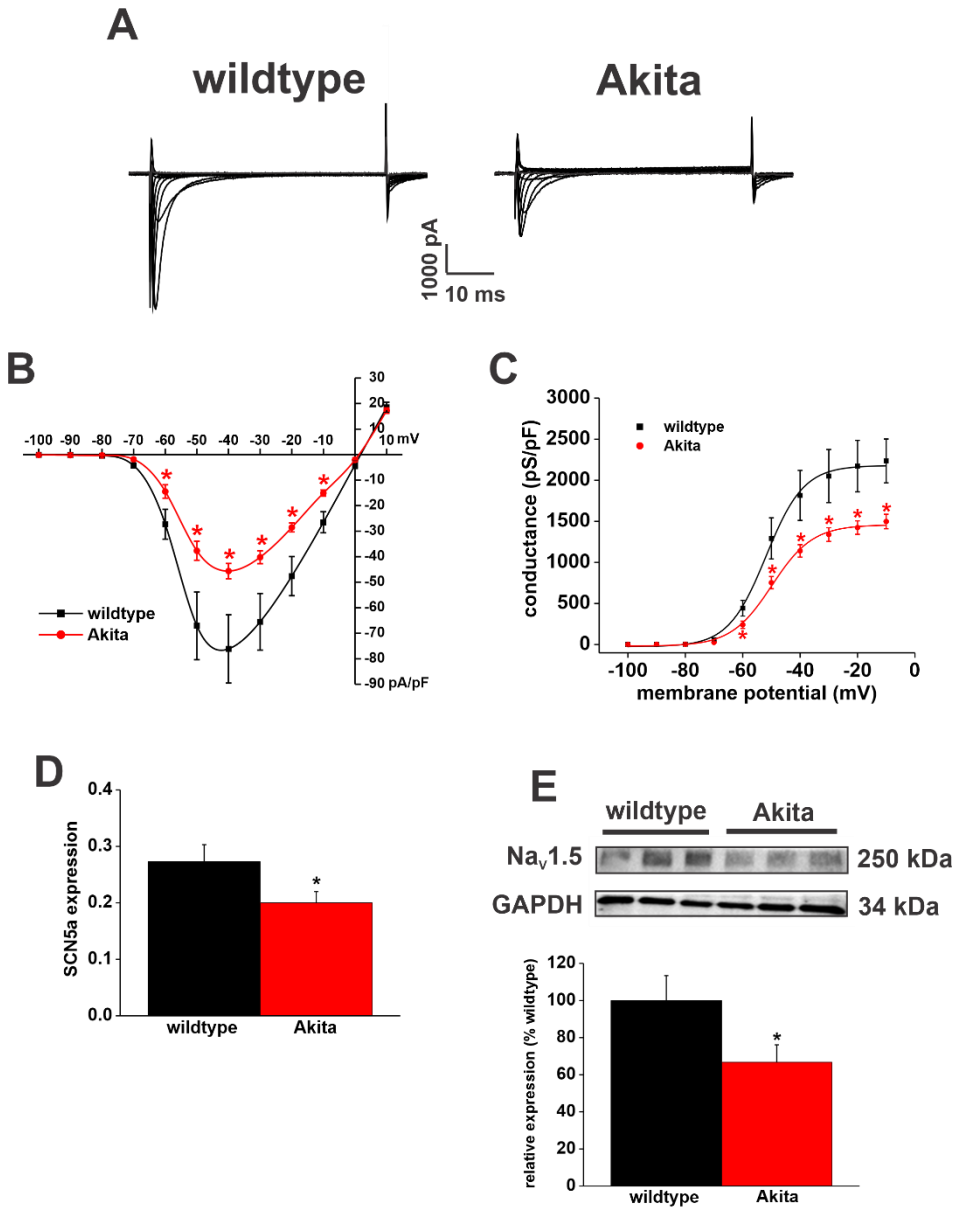

Figure S7. I_{Na} is reduced in left atrial myocytes in Akita mice. (*A*) Representative I_{Na} recordings in left atrial myocytes isolated from wildtype and Akita mice. Cell capacitances for these representative recordings was 42 pF for wildtype and 49 pF for Akita. (*B*) I_{Na} IV curves in left atrial myocytes isolated from wildtype and Akita mice. (*C*) I_{Na} activation curves in left atrial myocytes from wildtype and Akita mice. For left atrial myocytes n=5 for wildtype and 11 for Akita; *P<0.05 vs. wildtype at each membrane potential by two-way repeated measures ANOVA with Tukey's posthoc test. I_{Na} activation kinetics are summarized in Supplemental Table 13. (*D*) *SCN5a* gene expression in the right atrium in wildtype and Akita mice. *P<0.05 vs. wildtype by Student's t-test; n=15 wildtype and 17 Akita mice. (*E*) $Na_V1.5$ protein expression in the left atrium in wildtype and Akita mice. *P<0.05 vs. wildtype by Student's t-test, n=6 wildtype and 6 Akita mice.

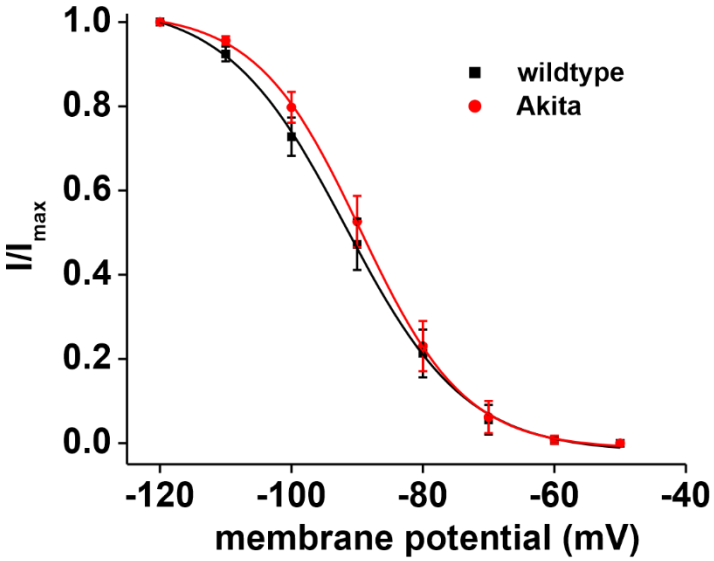

Figure S8: Steady state I_{Na} inactivation in Akita right atrial myocytes. I_{Na} inactivation curves for wildtype and Akita right atrial myocytes. There was no difference (*P*=0.341) in I_{Na} $V_{1/2(inact)}$ between wildtype (-91.3 ± 2.4 mV) and Akita (-88.9 ± 2.2 mV) mice. Data analyzed by Student's *t*-test; *n*=11 wildtype myocytes and 10 Akita myocytes.

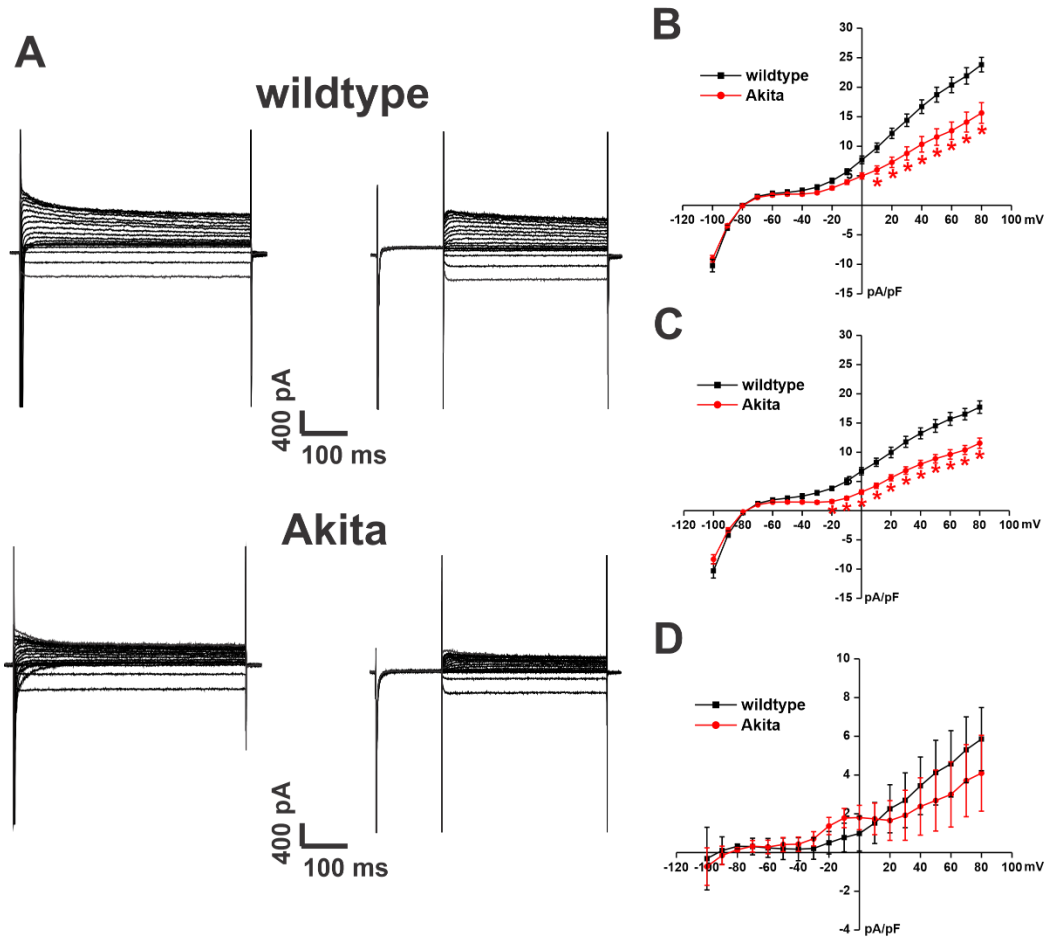

Figure S9. Repolarizing K^+ current is reduced in left atrial myocytes in Akita mice. (*A*) Representative K^+ current recordings in left atrial myocytes isolated from wildtype and Akita mice. The recordings on the left represent total I_K measured between -100 and +80 mV. The recordings on the right represent I_K measured between -100 and +80 mV following a pre-pulse to -40 mV to inactivate I_{to}. Cell capacitances for these representative recordings was 49 pF for wildtype and 43 pF for Akita. (*B*) I_K IV curves measured at the peak of the I_K recordings without the pre-pulse (recordings on the left in panel A) for left atrial myocytes isolated from wildtype and Akita mice. (*C*) I_K IV curves measured at the peak of the I_K recordings with the pre-pulse (recordings on the right in panel A) for left atrial myocytes isolated from wildtype and Akita mice. For panels *B* and *C* **P*<0.05 vs. wildtype at each membrane potential by two-way repeated measures ANOVA with Tukey's posthoc test. (*D*) I_K IV curves for the different current between *B* and *C*, which is a measure of I_{to}. There was no difference (*P*=0.73) in I_{to} density between wildtype and Akita. For panels *B*-*D* *n*=13 wildtype and 11 Akita left atrial myocytes.

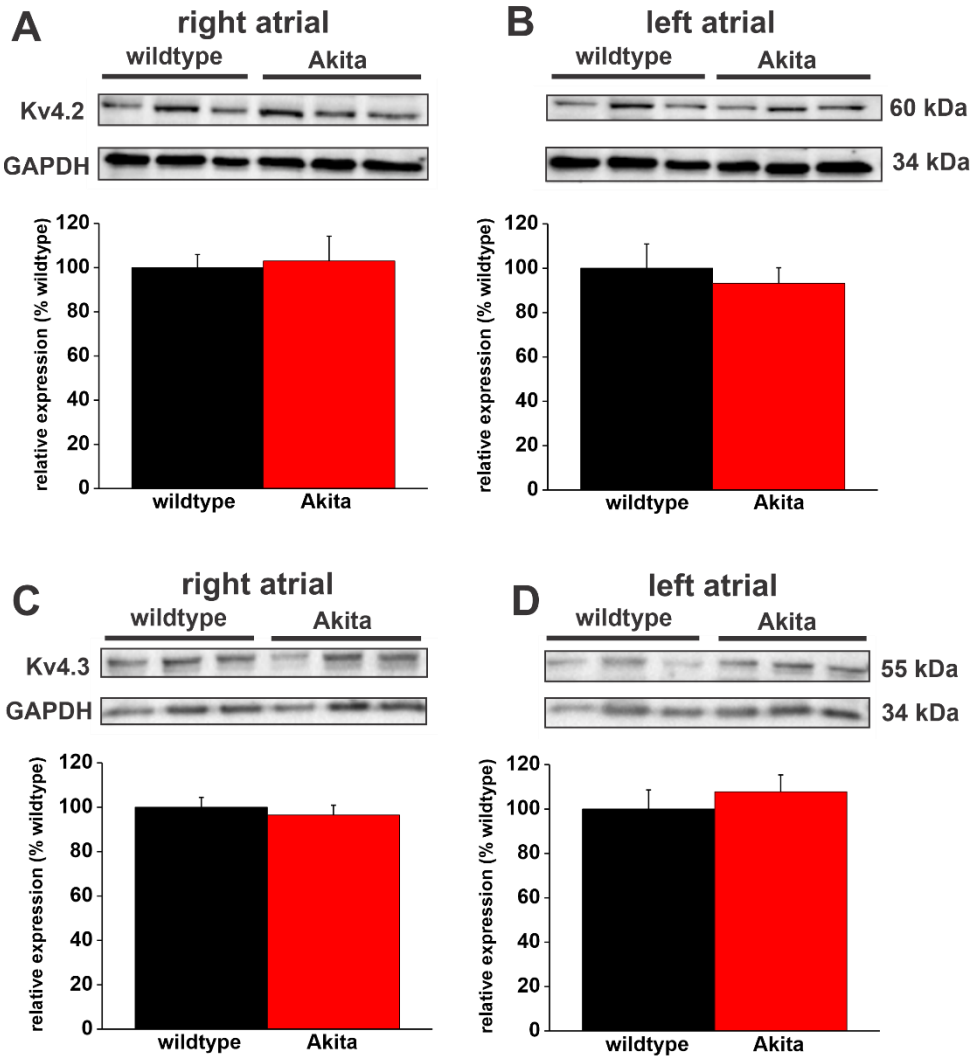

Figure S10. Protein expression of K_V4.2 and K_V4.3 in right and left atria. (*A*) Expression of K_V4.2 in the right atrium in wildtype and Akita mice. *P*=0.79 by Student's t-test, *n*=6 for wildtype and 6 for Akita. (*B*) Expression of K_V4.2 in the left atrium in wildtype and Akita mice. *P*=0.61 by Student's *t*-test, *n*=6 for wildtype and 6 for Akita. (*C*) Expression of K_V4.3 in the right atrium in wildtype and Akita mice. *P*=0.58 by Student's *t*-test, *n*=9 for wildtype and 9 for Akita. (*D*) Expression of K_V4.3 in the left atrium in wildtype and Akita mice. *P*=0.51 by Student's *t*-test, *n*=9 for wildtype and 9 for Akita.

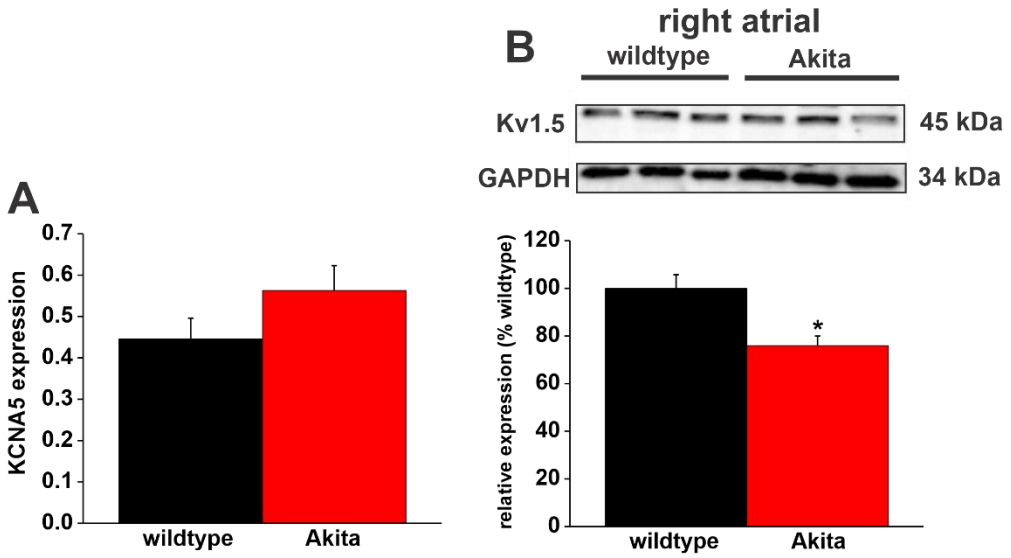

Figure S11. Atrial expression of KCNA5 gene and K_V1.5 protein in Akita mice. (*A*) Right atrial KCNA5 gene expression in wildtype and Akita mice. *P*=0.106; *n*=23 for wildtype and 15 for Akita. (*B*) Right atrial K_V1.5 expression was measured in wildtype and Akita mice. **P*<0.05 vs. wildtype by Student's *t*-test, *n*=9 for wildtype and 9 for Akita.

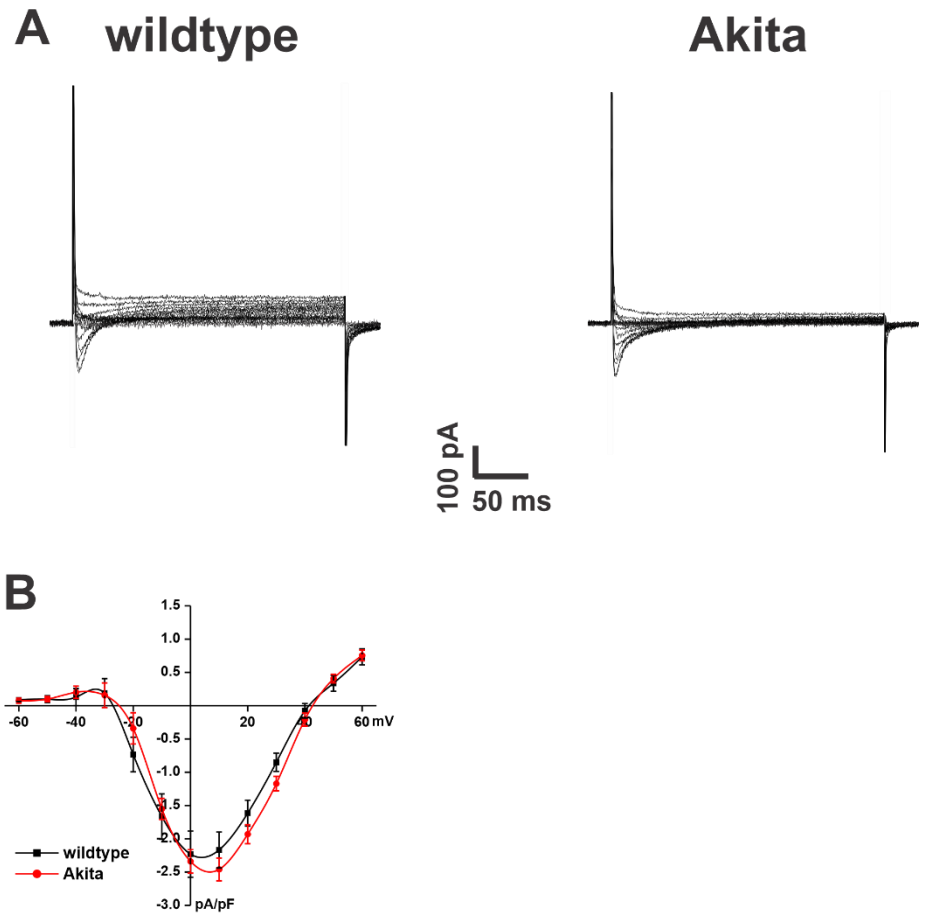

Figure S12. Measurement of atrial $I_{Ca,L}$ in Akita mice. (*A*) Representative $I_{Ca,L}$ recordings in isolated right atrial myocytes from wildtype and Akita mice. Cell capacitances for these representative recordings was 50 pF for wildtype and 41 pF for Akita. (*B*) $I_{Ca,L}$ IV curves in right atrial myocytes from wildtype and Akita mice; *n*=11 wildtype and 12 Akita right atrial myocytes. There was no difference (*P*=0.260) in $I_{Ca,L}$ between groups; data analyzed by two-way repeated measures ANOVA.

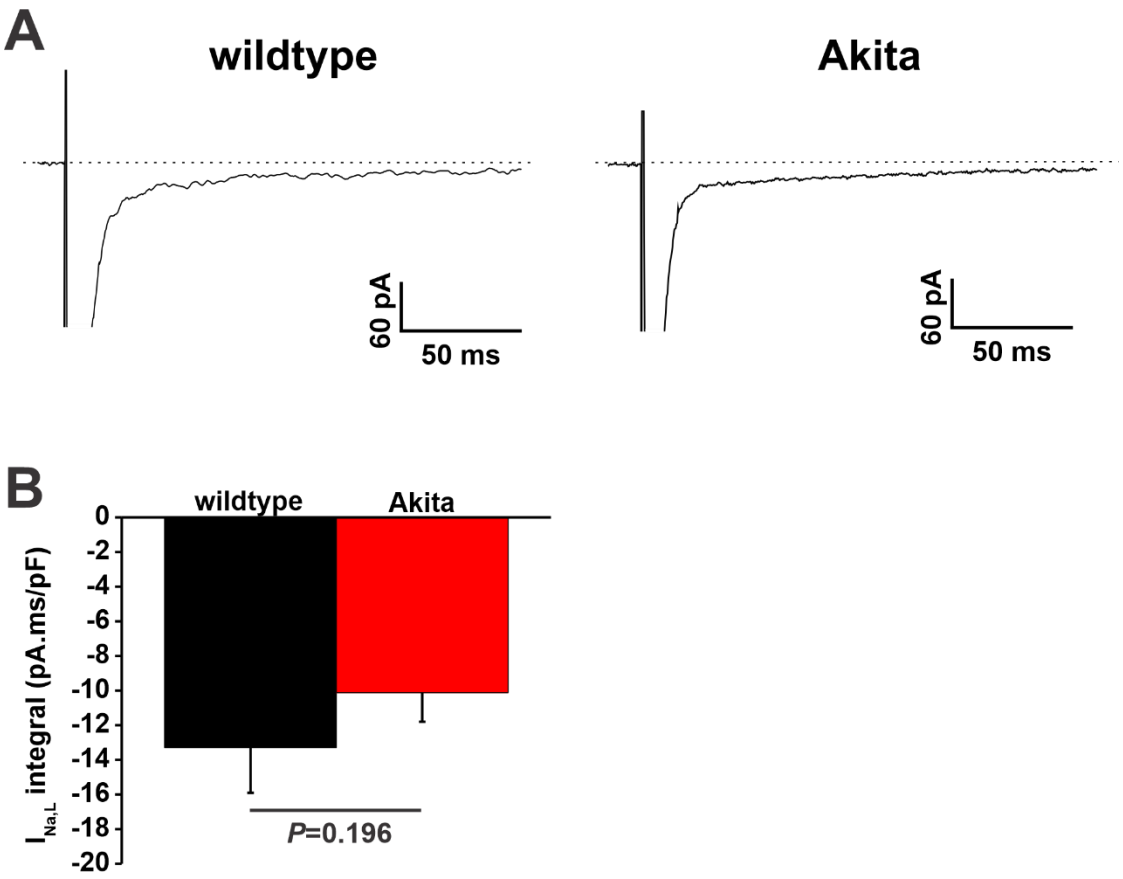

Figure S13: Late Na^+ current in Akita right atrial myocytes. (*A*) Representative $I_{Na,L}$ recordings from wildtype and Akita right atrial myocytes. Cell capacitances for these representative recordings was 38 pF for wildtype and 34 pF for Akita. (*B*) $I_{Na,L}$ (measured as an integral between 100 – 150 ms) in wildtype and Akita right atrial myocytes. Data analyzed by Student's *t*-test, *n*=10 wildtype and 9 Akita atrial myocytes.

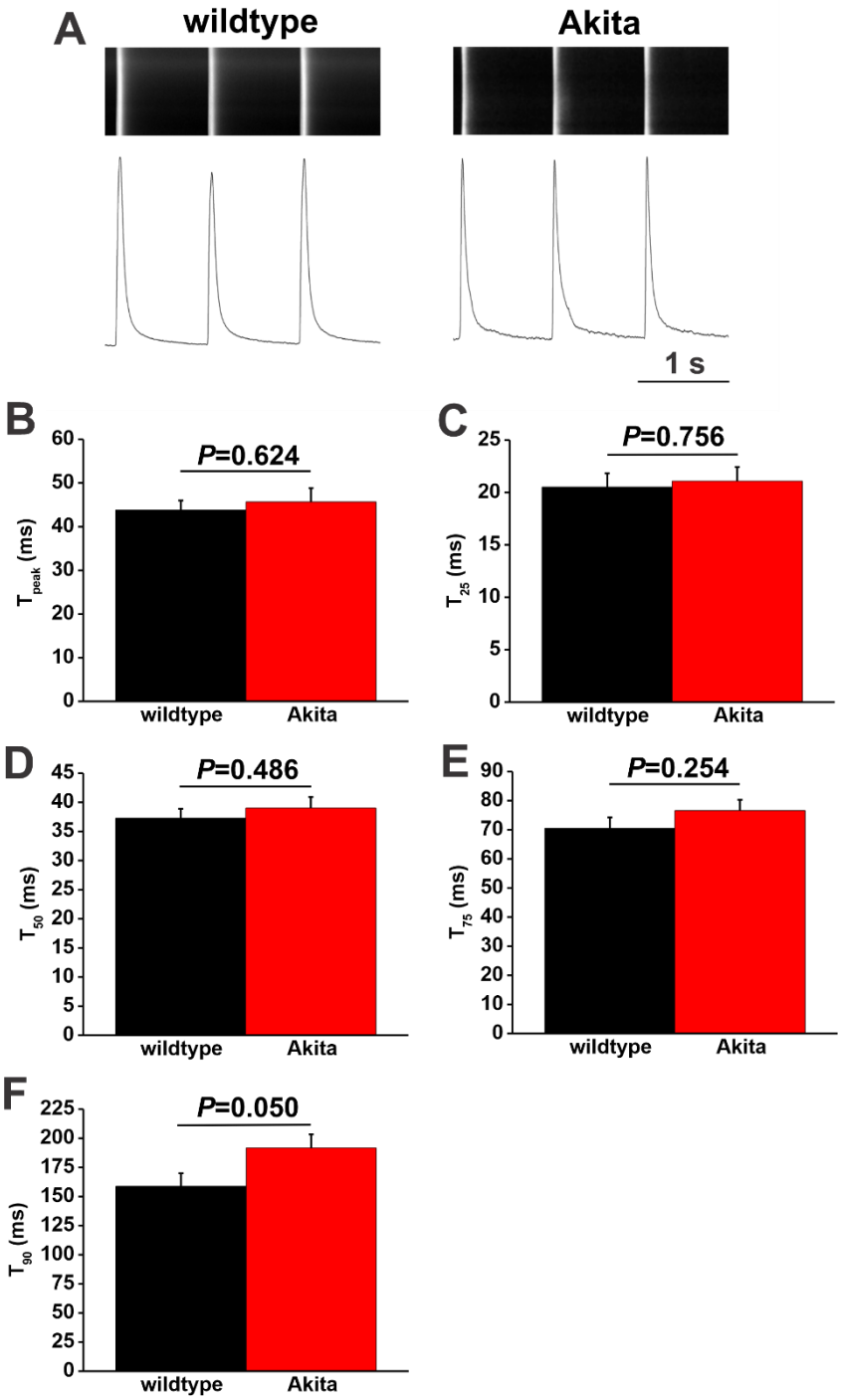

Figure S14: Calcium transient morphology in Akita atrial myocytes. (*A*) Representative confocal line scans and stimulated calcium transients in atrial myocytes from wildtype and Akita mice. (*B*) Summary of time to peak (T_{peak}) in wildtype and Akita atrial myocytes. (*C-E*) Calcium transient duration at 25% (T_{25}, panel *C*), 50% (T_{50}, panel *D*), 75% (T_{75}, panel *E*) and 90% (T_{90}, panel *E*) decay times. Data analyzed by Student's *t*-test; *n*=19 wildtype and 20 Akita atrial myocytes.

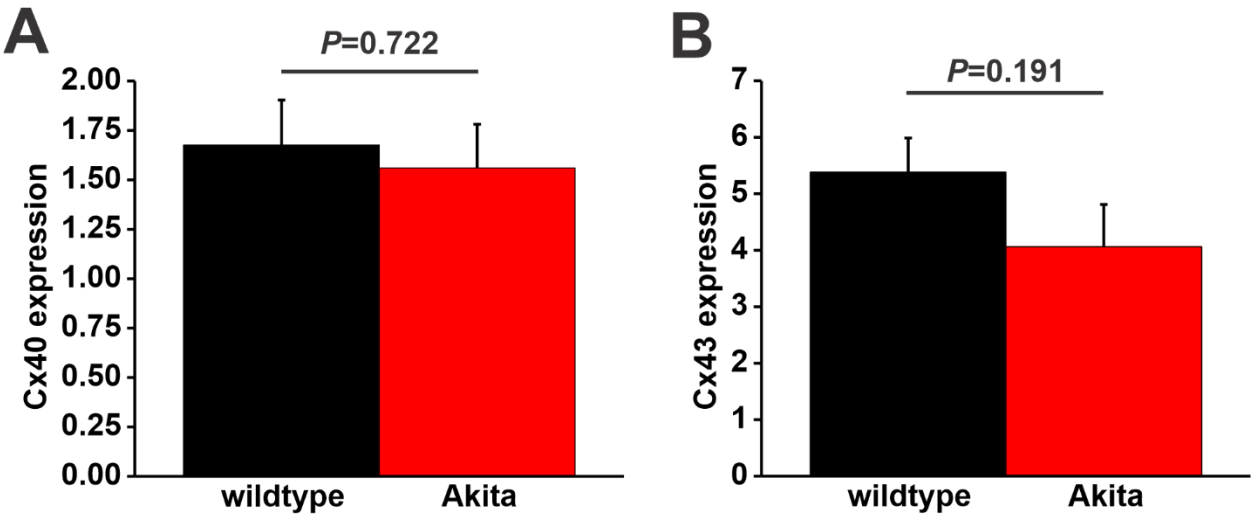

Figure S15: Expression of connexin 40 and connexin 43 in the right atrium in Akita mice. (*A*) Expression of *GJA5* (encodes Cx40) mRNA in wildtype and Akita right atria. (*B*) Expression of *GJA1* (encodes Cx43) mRNA in wildtype and Akita right atria. Data analyzed by Student's t-test; *n*=8 right atria for each group.

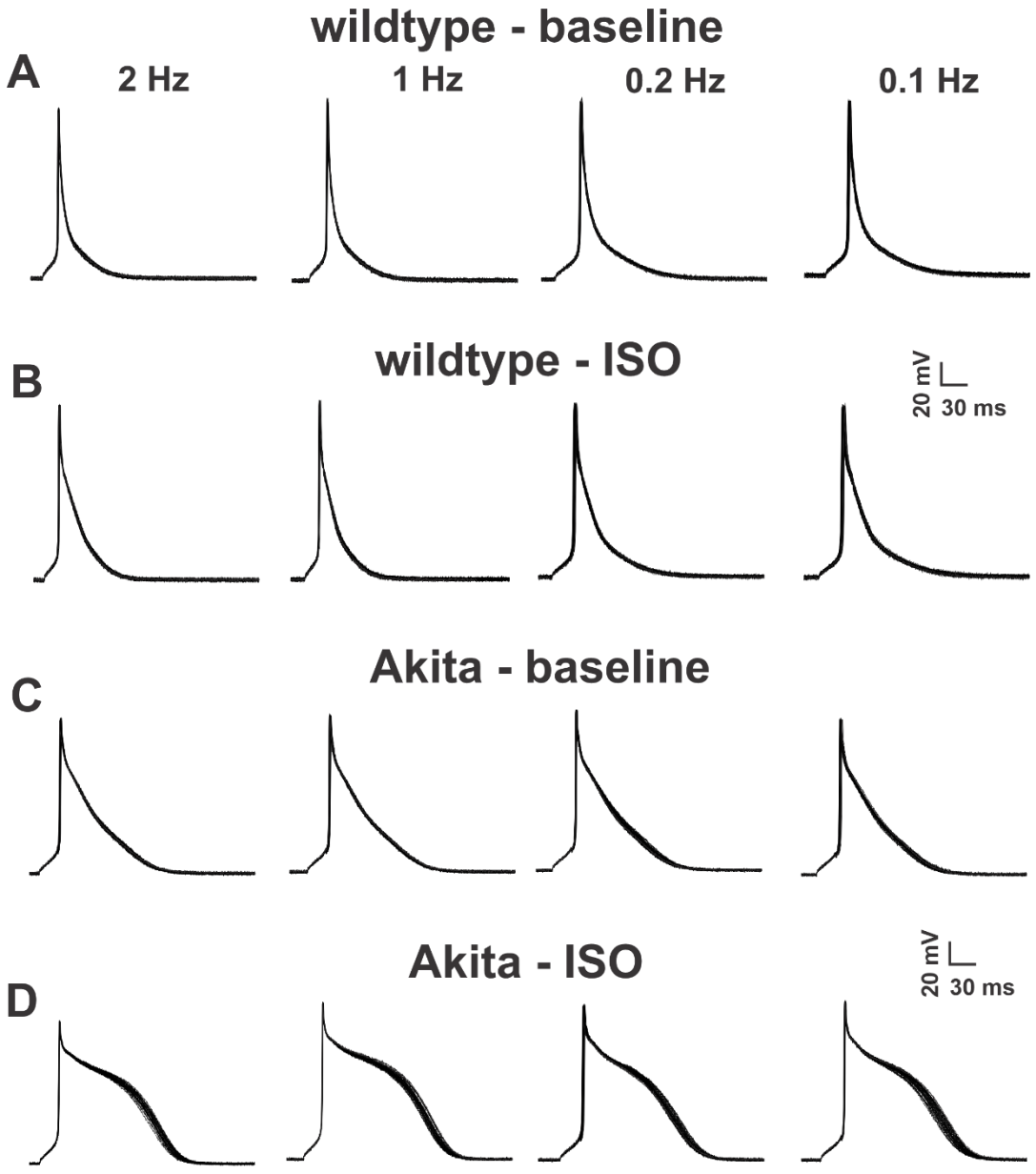

Figure S16: Assessment of early afterdepolarizations in Akita right atrial myocytes. EAD susceptibility was assessed by recording APs at pacing frequencies of 2, 1, 0.2 and 0.1 Hz in baseline conditions and in the presence of isoproterenol (ISO; 1 µM) in wildtype and Akita right atrial myocytes. Each panel contains an overlay of 30 successive APs in each condition. No EADs were observed.

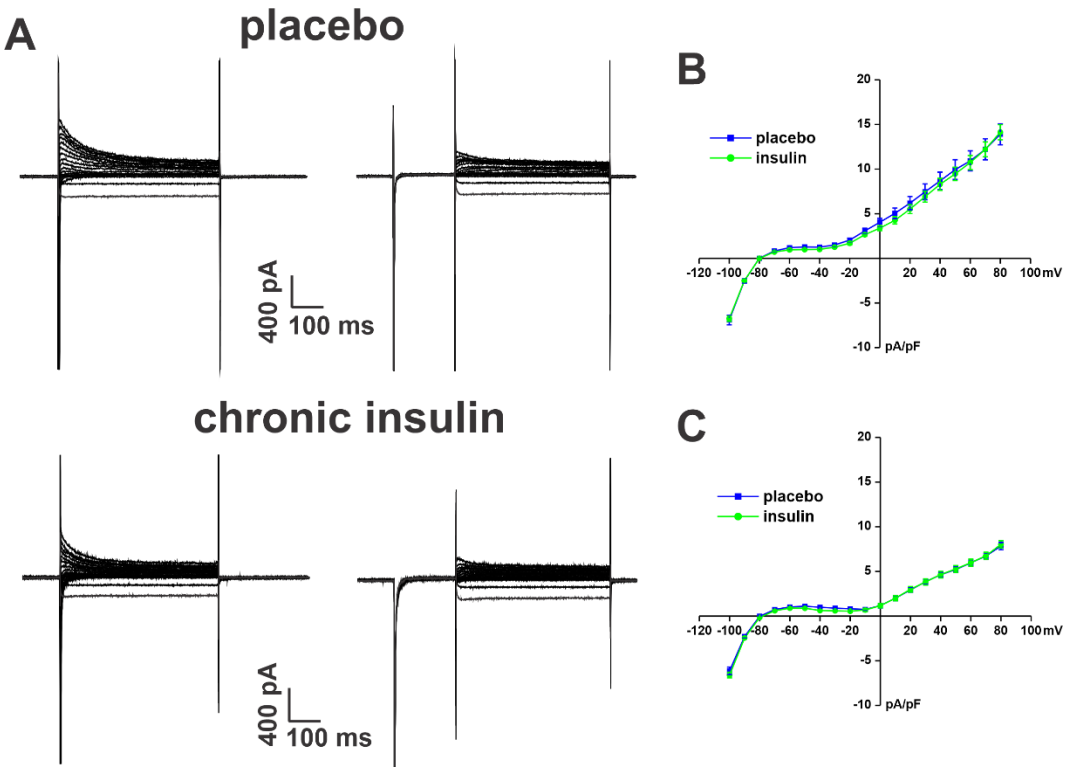

Figure S17. Chronic insulin treatment has no effect on K^+ currents in Akita mice. (*A*) Representative K^+ current recordings in right atrial myocytes from Akita mice treated chronically with insulin or placebo. The recordings on the left represent total I_K measured between -100 and +80 mV. The recordings on the right represent I_K measured between -100 and +80 mV following a pre-pulse to -40 mV to inactivate I_{to}. Cell capacitances for these representative recordings was 31 pF for wildtype and 38 pF for Akita. (*B*) I_K IV curves measured at the peak of the I_K recordings without the pre-pulse (recordings on the left in panel A) for right atrial myocytes isolated from insulin or placebo treated Akita mice. There was no difference in I_K density between groups (P=0.61 by two-way repeated measures ANOVA with Tukey's posthoc test). (*C*) I_K IV curves measured at the peak of the I_K recordings with the pre-pulse (recordings on the right in panel A) for right atrial myocytes isolated from insulin or placebo treated Akita mice. There was no difference in I_K density between groups (P=0.67 by two-way repeated measures ANOVA with Tukey's posthoc test); n=18 myocytes for placebo and 21 myocytes for chronic insulin.

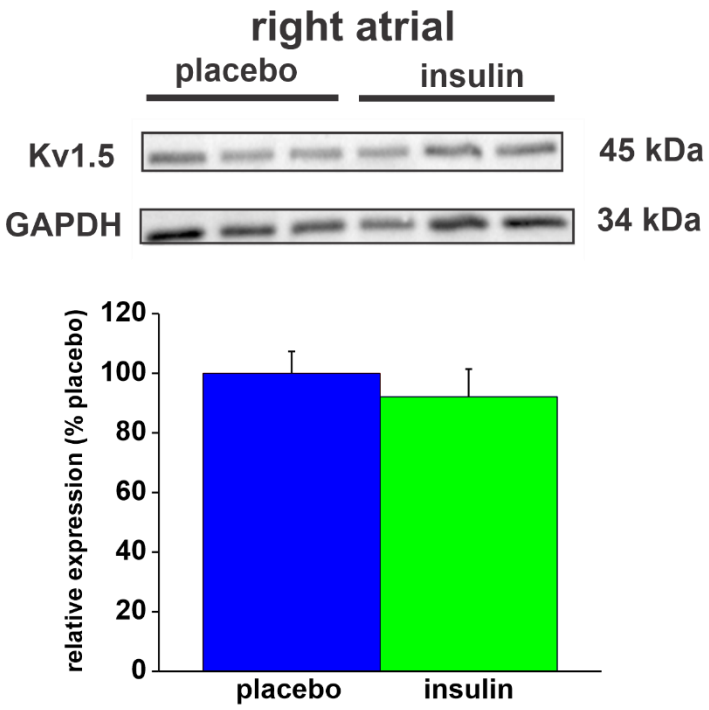

Figure S18. Protein expression of K_V1.5 in Akita mice treated chronically with insulin. Right atrial K_V1.5 was measured following chronic insulin or placebo treatment. *P*=0.56 by Student's *t*-test, *n*=12 for placebo and 12 for chronic insulin.

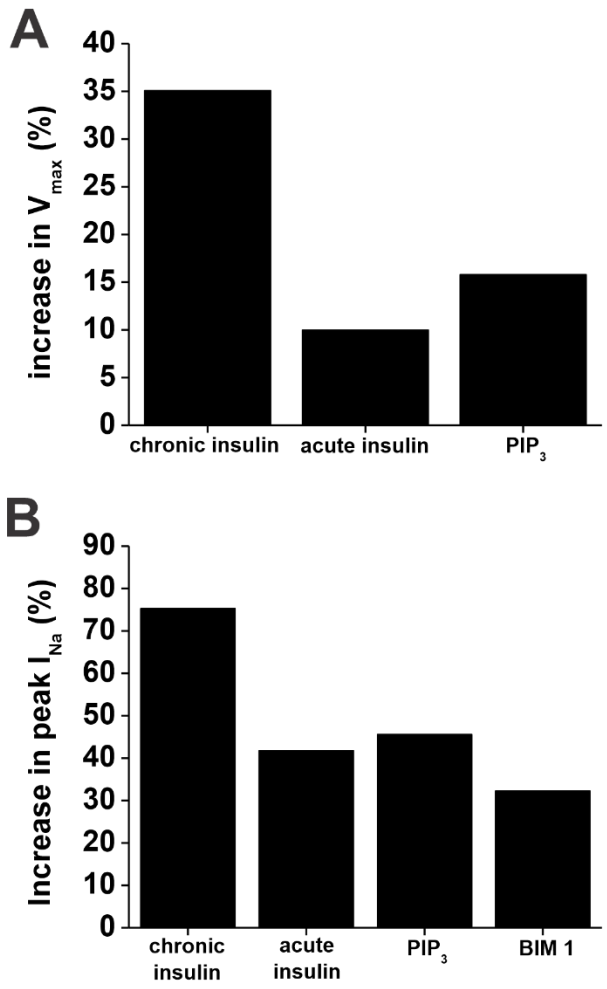

Figure S19. Comparison of the magnitude of the effects of drug treatments on AP V_{max} (*A*) and peak atrial I_{Na} (*B*) in Akita mice. Percent changes were measured relative to the specific control group for each treatment as outlined in the manuscript.

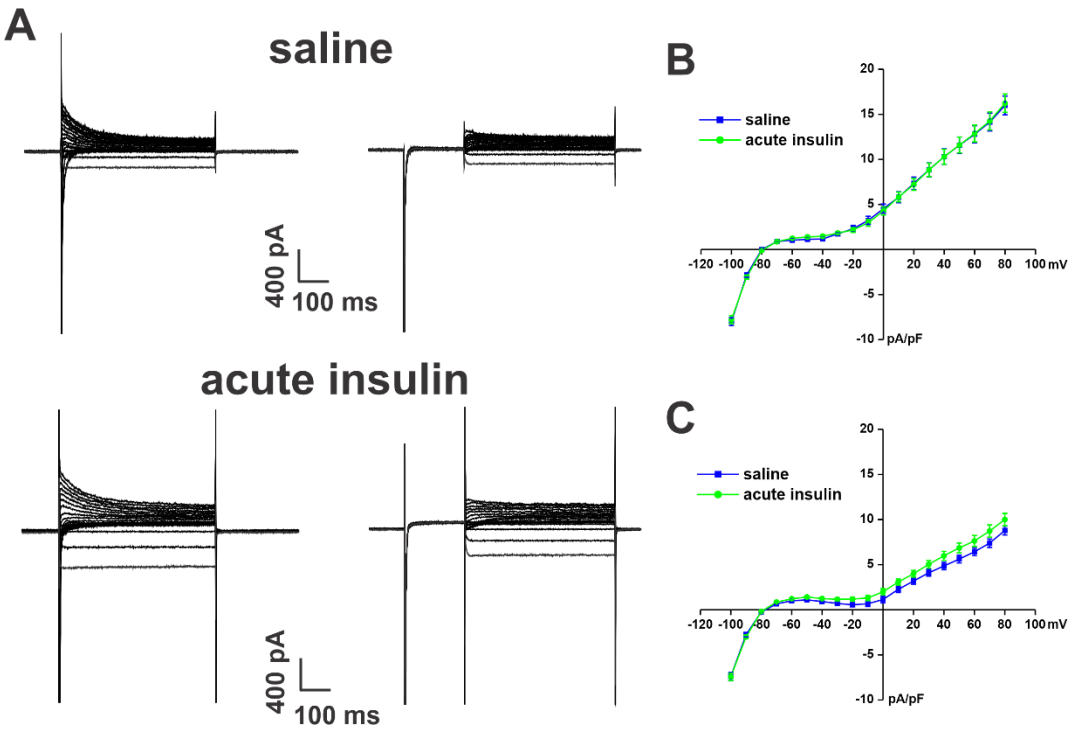

Figure S20. Acute insulin treatment has no effect on K^+ currents in Akita mice. (*A*) Representative K^+ current recordings in right atrial myocytes from Akita mice acutely injected with insulin or saline as a control. The recordings on the left represent total I_K measured between -100 and +80 mV. The recordings on the right represent I_K measured between -100 and +80 mV following a pre-pulse to -40 mV to inactivate I_{to}. Cell capacitances for these representative recordings was 35 pF for wildtype and 41 pF for Akita. (*B*) I_K IV curves measured at the peak of the I_K recordings without the pre-pulse (recordings on the left in panel *A*) for right atrial myocytes isolated from insulin or saline treated Akita mice. There was no difference in I_K density between groups (P=0.97 by two-way repeated measures ANOVA with Tukey's posthoc test). (*C*) I_K IV curves measured at the peak of the I_K recordings with the pre-pulse (recordings on the right in panel A) for right atrial myocytes isolated from insulin or saline treated Akita mice. There was no difference in I_K density between groups (P=0.08 by two-way repeated measures ANOVA with Tukey's posthoc test); n=20 myocytes for saline and 20 myocytes for acute insulin.

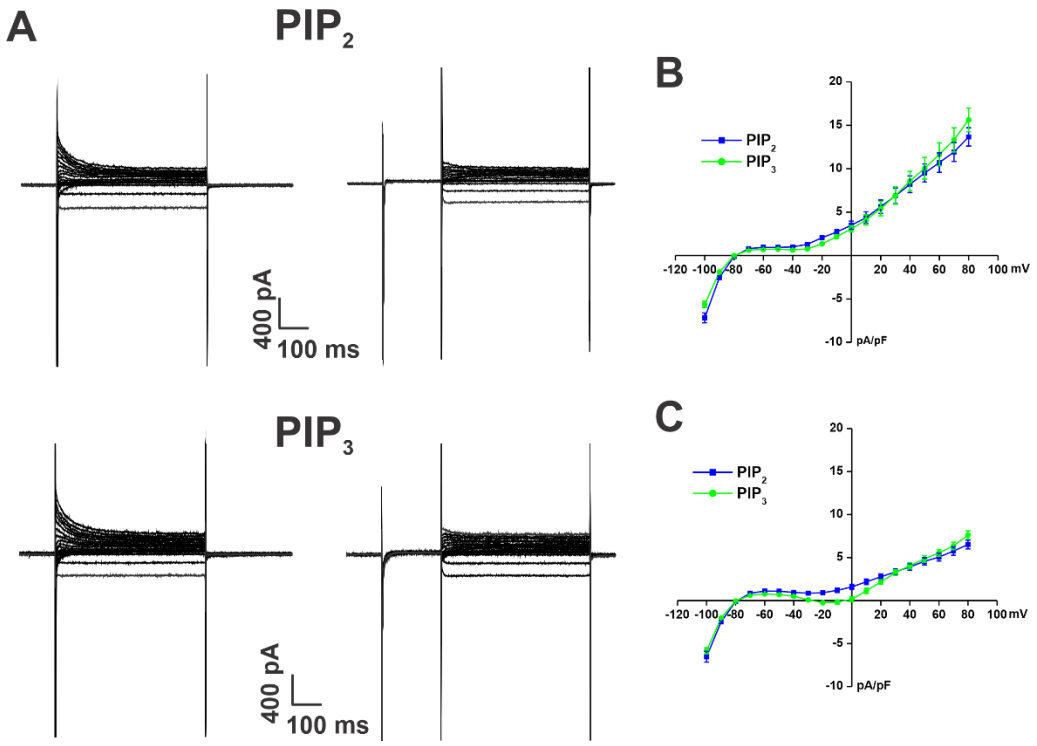

Figure S21. PIP_3 has no effect on K^+ currents in Akita mice. (*A*) Representative K^+ current recordings in right atrial myocytes from Akita mice dialyzed with PIP_3 (1 μM) or PIP_2 (1 μM). Data are from cells dialyzed for 10 min with phospholipids. The recordings on the left represent total I_K measured between -100 and +80 mV. The recordings on the right represent I_K measured between -100 and +80 mV following a pre-pulse to -40 mV to inactivate I_{to}. Cell capacitances for these representative recordings was 44 pF for wildtype and 52 pF for Akita. (*B*) I_K IV curves measured at the peak of the I_K recordings without the pre-pulse (recordings on the left in panel *A*) for Akita right atrial myocytes dialyzed with PIP_3 or PIP_2. There was no difference in I_K density between groups (P=0.76 by two-way repeated measures ANOVA with Tukey's posthoc test). (*C*) I_K IV curves measured at the peak of the I_K recordings with the pre-pulse (recordings on the right in panel A) for Akita right atrial myocytes dialyzed with PIP_3 or PIP_2. There was no difference in I_K density between groups (P=0.39 by two-way repeated measures ANOVA with Tukey's posthoc test); n=9 myocytes for PIP_2 and 10 myocytes for PIP_3.

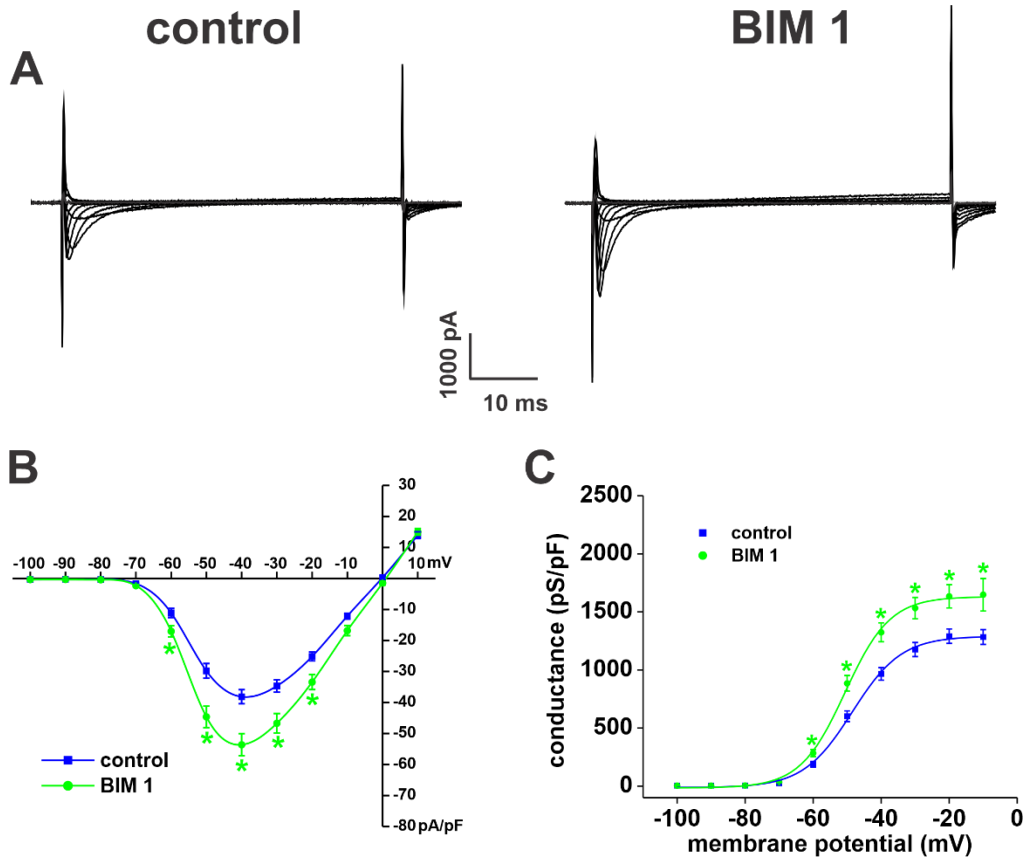

Figure S22. Effects of protein kinase C inhibition in I_{Na} in Akita mice. (*A*) Representative I_{Na} recordings in right atrial myocytes from Akita mice following dialysis with the PKC inhibitor BIM 1 (1 μM) compared to control Akita myocytes. Cell capacitances for these representative recordings was 34 pF for wildtype and 39 pF for Akita. (*B*) I_{Na} IV curves for right atrial myocytes from untreated Akita mice in control conditions and after dialysis with BIM 1. (C) I_{Na} activation curves for right atrial myocytes from Akita mice in control conditions and after dialysis with BIM 1. For panels *B* and *C* **P*<0.05 vs. control by two-way repeated measures ANOVA with Tukey's posthoc test; *n*=18 myocytes for control and 20 myocytes for BIM 1. Refer to Supplemental Table 13 for additional analysis of I_{Na} activation kinetics.

Table S1: Duration of arrhythmia in wildtype and Akita mice that were induced into atrial fibrillation

	wildtype	Akita
< 5s	100% (2/2)	15% (2/13)
5-30 s	0% (0/2)	62% (8/13)
>30 s	0% (0/2)	23% (3/13)

Numbers in parentheses indicate the number of mice in each group.

Table S2: Duration of arrhythmia in wildtype mice treated with STZ that were induced into atrial fibrillation

	veh	STZ
< 5s	100% (3/3)	37.5% (3/8)
5-30 s	0% (0/3)	37.5% (3/8)
>30 s	0% (0/3)	25% (2/8)

Numbers in parentheses indicate the number of mice in each group. veh, vehicle; STZ, streptozotocin.

Table S3: Duration of arrhythmia in Akita mice treated chronically with insulin or placebo that were induced into atrial fibrillation

	Placebo	chronic insulin
< 5s	54% (7/13)	83% (5/6)
5-30 s	38% (5/13)	17% (1/6)
>30 s	8% (1/13)	0% (0/6)

Mice were treated with insulin (or placebo) for 4 weeks prior to investigation. Numbers in parentheses indicate the number of mice in each group.

Table S4: Duration of arrhythmia in Akita mice treated acutely with insulin or saline that were induced into atrial fibrillation

	Saline	acute insulin
< 5s	17% (1/6)	20% (1/5)
5-30 s	67% (4/6)	60% (3/5)
>30 s	17% (1/6)	20% (1/5)

Mice were treated acutely with insulin (or saline) immediately prior to investigation. Numbers in parentheses indicate the number of mice in each group.

Table S5: ECG intervals in wildtype and Akita mice

	Wildtype	Akita	*P* value
Heart rate (beats/min)	556 ± 21	496 ± 13*	0.022
R-R interval (ms)	108.7 ± 3.7	121.7 ± 3.4*	0.024
P wave (ms)	26.7 ± 1.0	38.1 ± 1.3*	<0.001
P-R interval (ms)	46.3 ± 1.7	54.7 ± 1.6*	0.003

Data are means ± SEM; *n* = 7-10 mice per group. *P<0.05 vs. wildtype by Student's *t*-test.

Table S6: ECG intervals in wildtype mice treated with STZ

	veh	STZ	*P* value
Heart rate (beats/min)	520 ± 9	508 ± 14	0.566
R-R interval (ms)	116.1 ± 2.2	120.0 ± 3.8	0.375
P wave (ms)	25.3 ± 0.5	27.7 ± 0.7*	0.010
P-R interval (ms)	45.1 ± 0.8	49.0 ± 1.5	0.069

Data are means ± SEM; *n* = 17-19 mice per group. *P<0.05 vs. wildtype by Student's *t*-test.

Table S7: ECG intervals in placebo and chronic insulin treated Akita mice

	placebo	chronic insulin	*P* value
Heart rate (beats/min)	501 ± 10	544 ± 11*	0.007
R-R interval (ms)	120.9 ± 2.9	111.3 ± 2.4*	0.005
P wave (ms)	33.0 ± 1.3	28.7 ± 1.0*	0.023
P-R interval (ms)	55.8 ± 2.2	51.4 ± 1.7	0.07

Mice were treated with insulin (or placebo) for 4 weeks prior to investigation. Data are means ± SEM; *n*=21-22 mice per group. *P<0.05 vs. placebo by Student's *t*-test.

Table S8: ECG intervals in saline and acute insulin treated Akita mice

	saline	acute insulin	*P* value
Heart rate (beats/min)	507 ± 28	499 ± 9	0.32
R-R interval (ms)	121.3 ± 8.7	120.6 ± 2.3	0.32
P wave (ms)	38.7 ± 0.71	36.2 ± 0.8*	0.03
P-R interval (ms)	57.0 ± 1.8	56.9 ± 2.3	0.95

Mice were treated acutely with insulin (or saline) immediately prior to investigation. Data are means ± SEM; *n*=7-8 mice per group. *P<0.05 vs. saline by Student's *t*-test.

Table S9: Echocardiographic measurements in wildtype and Akita mice

	Wildtype	Akita	*P* value
LVAWd (mm)	0.89 ± 0.02	0.79 ± 0.05*	0.024
LVPWd (mm)	0.87 ± 0.02	0.82 ± 0.03	0.576
LVIDd (mm)	4.72 ± 0.12	4.32 ± 0.08*	0.003
LVAWs (mm)	1.35 ± 0.04	1.24 ± 0.06	0.056
LVPWs (mm)	1.19 ± 0.02	1.16 ± 0.04	0.768
LVIDs (mm)	3.42 ± 0.12	3.00 ± 0.09*	0.011
EF (%)	53.39 ± 2.1	58.08 ± 1.7	0.182
LA $area_{max}$ (mm^2)	6.51 ± 0.3	7.36 ± 0.5*	0.042
LA $area_{min}$ (mm^2)	4.20 ± 0.3	4.63 ± 0.4	0.320
RA $area_{max}$ (mm^2)	5.55 ± 0.3	6.02 ± 0.4	0.294
RA $area_{min}$ (mm^2)	3.27 ± 0.22	4.21 ± 0.7	0.310

LVAW, left ventricular anterior wall thickness; LVPW, left ventricular posterior wall thickness; LVID, left ventricular internal diameter. LVAW, LVPW and LVID measurements were made during systole (s) and diastole (d). EF, ejection fraction; LA $area_{max}$, maximum left atrial area; LA $area_{min}$, minimum left atrial area. RA $area_{max}$, maximum right atrial area; RA $area_{min}$, minimum right atrial area. Data are means ± SEM; *n* = 11 mice per group. **P*<0.05 vs. wildtype by Student's *t*-test.

Table S10: Action potential parameters in right atrial myocytes from wildtype and Akita mice

	wildtype	Akita	*P* value
RMP (mV)	-78.2 ± 0.2	-77.7 ± 0.3	0.116
V_{max} (V/s)	172.9 ± 6.0	135.7 ± 6.9*	<0.001
OS (mV)	57.5 ± 2.3	46.2 ± 2.5*	0.002
APD_{50} (ms)	9.7 ± 1.3	14.3 ± 1.5*	0.022
APD_{70} (ms)	19.5 ± 2.4	26.4 ± 2.7*	0.044
APD_{90} (ms)	41.3 ± 3.2	51.3 ± 3.6*	0.047

RMP, resting membrane potential; V_{max}, AP upstroke velocity; OS, overshoot; APD_{50}, AP duration at 50% repolarization; APD_{70}, AP duration at 70% repolarization; APD_{90}, AP duration at 90% repolarization. **P*<0.05 vs wildtype by Student's *t*-test; *n*=18 wildtype and 16 Akita myocytes.

Table S11: Action potential parameters in left atrial myocytes from wildtype and Akita mice

	wildtype	Akita	*P* value
RMP (mV)	-78.0 ± 0.3	-77.8 ± 0.3	0.634
V_{max} (V/s)	168.1 ± 6.6	141.2 ± 5.8*	0.036
OS (mV)	53.8 ± 3.0	43.6 ± 5.8*	0.009
APD_{50} (ms)	9.1 ± 0.8	16.4 ± 1.3*	<0.001
APD_{70} (ms)	17.0 ± 1.4	29.7 ± 2.3*	<0.001
APD_{90} (ms)	36.4 ± 2.6	55.5 ± 4.5*	0.001

RMP, resting membrane potential; V_{max}, AP upstroke velocity; OS, overshoot; APD_{50}, AP duration at 50% repolarization; APD_{70}, AP duration at 70% repolarization; APD_{90}, AP duration at 90% repolarization. **P*<0.05 vs wildtype by Student's *t*-test; *n*=12 wildtype and 11 Akita myocytes.

Table S12: Action potential parameters in ventricular myocytes from wildtype and Akita mice

	wildtype	Akita	*P* value
RMP (mV)	-80.4 ± 0.4	-80.7 ± 0.3	0.663
V_{max} (V/s)	185.4 ± 7.3	177.3 ± 9.6	0.540
OS (mV)	60.4 ± 3.1	67.9 ± 2.2	0.08
APD_{50} (ms)	2.7 ± 0.1	4.7 ± 0.9*	0.04
APD_{70} (ms)	5.0 ± 0.3	9.1 ± 1.9*	0.04
APD_{90} (ms)	15.0 ± 1.1	22.5 ± 3.2*	0.03

RMP, resting membrane potential; V_{max}, AP upstroke velocity; OS, overshoot; APD_{50}, AP duration at 50% repolarization; APD_{70}, AP duration at 70% repolarization; APD_{90}, AP duration at 90% repolarization. **P*<0.05 vs wildtype by Student's *t*-test; *n*=8 wildtype and 11 Akita ventricular myocytes.

Table S13: I_{Na} kinetics

	G_{max} (pS/pF)	P value	$V_{1/2(act)}$ (mV)	P value	k (mV)	P value
Wildtype right atrial	1973.2 ± 74.3	<0.001	-51.5 ± 0.6	0.009	5.1 ± 0.1	<0.001
Akita right atrial	1232.9 ± 85.9*		-48.9 ± 0.7*		6.2 ± 0.2*	
Wildtype left atrial	2095.5 ± 300.1	0.009	-52.4 ± 1.5	<0.05	5.7 ± 0.4	0.82
Akita left atrial	1412.0 ± 79.1*		-49.7 ± 1.2*		5.8 ± 0.3	
Akita placebo	927.1 ± 86.9	<0.001	-47.7 ± 0.8	0.71	4.4 ± 0.2	0.78
Akita insulin (chronic)	1589.5 ± 134.1*		-48.2 ± 1.2		4.3 ± 0.5	
Akita saline	1214.1 ± 37.8	0.01	-49.7 ± 1.2	0.86	6.1 ± 0.3	0.11
Akita insulin (acute)	1535. 5 ± 60.3*		-51.0 ± 0.6		5.6 + 0.2	
Akita PIP_2	863.0 ± 98.8	<0.001	-48.8 ± 0.9	0.61	5.6 ± 0.3	0.58
Akita PIP_3	1359.3 ± 79.1*		-48.9 ± 0.7		5.8 ± 0.2	
Akita control	1252.5 ± 60.8	0.02	-48.9 ± 0.8	0.006	6.2 ± 0.1	0.07
Akita BIM1	1543.5 ± 96.9*		-51.4 ± 0.5*		5.6 ± 0.1	

G_{max}, maximum conductance, $V_{1/2(act)}$, voltage at which 50% of channels are activated; k, slope factor. **P*<0.05 vs control value as indicated in the table cell immediately above, *n* values are as reported in figure legends for each experimental group in the main manuscript. Data analyzed by Student's *t*-test.

Table S14: Action potential parameters in right atrial myocytes from Akita mice treated chronically with insulin

	placebo	chronic insulin	*P* value
RMP (mV)	-78.1 ± 0.2	-78.9 ± 0.1*	0.002
V_{max} (V/s)	126.4 ± 4.4	170.8 ± 2.7*	<0.001
OS (mV)	46.6 ± 2.6	56.3 ± 1.2*	<0.001
APD_{50} (ms)	18.8 ± 3.4	18.7 ± 2.0	0.560
APD_{70} (ms)	33.1 ± 5.5	35.1 ± 2.9	0.733
APD_{90} (ms)	61.5 ± 8.0	67.2 ± 4.6	0.518

RMP, resting membrane potential; V_{max}, AP upstroke velocity; OS, overshoot; APD_{50}, AP duration at 50% repolarization; APD_{70}, AP duration at 70% repolarization; APD_{90}, AP duration at 90% repolarization. *P<0.05 vs placebo by Student's t-test; n=19 placebo and 14 insulin treated myocytes.

Table S15: Action potential parameters in right atrial myocytes from Akita mice treated acutely with insulin

	saline	acute insulin	*P* value
RMP (mV)	-77.7 ± 0.4	-77.7 ± 0.3	0.567
V_{max} (V/s)	137.4 ± 4.1	151.2 ± 5.2*	0.03
OS (mV)	49.3 ± 1.9	49.0 ± 1.7	0.607
APD_{50} (ms)	14.6 ± 1.0	16.5 ± 2.8	0.766
APD_{70} (ms)	28.6 ± 2.0	29.7 ± 4.4	0.620
APD_{90} (ms)	58.3 ± 3.6	53.3 ± 5.5	0.423

RMP, resting membrane potential; V_{max}, AP upstroke velocity; OS, overshoot; APD_{50}, AP duration at 50% repolarization; APD_{70}, AP duration at 70% repolarization; APD_{90}, AP duration at 90% repolarization. *P<0.05 vs saline by Student's t-test; n=14 saline and 18 insulin treated myocytes.

Table S16: Action potential parameters in right atrial myocytes from Akita mice treated PIP_3

	PIP_2	PIP_3	*P* value
RMP (mV)	-78.3 ± 0.2	-79.2 ± 0.2*	0.015
V_{max} (V/s)	138.5 ± 6.8	160.4 ± 9.5*	0.039
OS (mV)	53.5 ± 3.4	48.9 ± 2.6	0.286
APD_{50} (ms)	12.4 ± 1.8	13.0 ± 2.0	0.194
APD_{70} (ms)	26.5 ± 3.3	27.5 ± 4.1	0.194
APD_{90} (ms)	56.9 ± 4.9	64.2 ± 6.2	0.052

RMP, resting membrane potential; V_{max}, AP upstroke velocity; OS, overshoot; APD_{50}, AP duration at 50% repolarization; APD_{70}, AP duration at 70% repolarization; APD_{90}, AP duration at 90% repolarization. *P<0.05 vs PIP_2 by Student's t-test; n=7 PIP_2 and 8 PIP_3 treated myocytes.

Supplemental Table 17: Quantitative PCR primers

Gene	Gene product	Primer Sequence (5'→ 3')	Amplicon length (bp)
SCN5a	$Na_v1.5$	Forward: GGAGTACGCCGACAAGATGT Reverse: ATCTCGGCAAAGCCTAAGGT	171
KCNA5	$K_v1.5$	Forward: TTATTCTTATGGCTGACGAGTGC Reverse: AAGGCACCAATAGTACATCCCAG	204
GJA5	Cx40	Forward: CACAGTCATCGGCAAGGTCT Reverse: ATGGTATCGCACCGGAAGTC	117
GJA1	Cx43	Forward: CCAAGGAGTTCCACCACTTTG Reverse: CCATGTCTGGGCACCTCTCT	70
GAPDH	GAPDH	Forward: AATGGGGTGAGGCCGGTGCT Reverse: CACCCTTCAAGTGGGCCCCG	87

References

1. Yoshioka M, Kayo T, Ikeda T, Koizumi A, A novel locus, Mody4, distal to D7Mit189 on chromosome 7 determines early-onset NIDDM in nonobese C57BL/6 (Akita) mutant mice. *Diabetes.* **46,** 887-894 (1997).
2. Krishnaswamy PS*, et al.*, Altered parasympathetic nervous system regulation of the sinoatrial node in Akita diabetic mice. *J Mol Cell Cardiol.* **82,** 125-135 (2015).
3. Bugger H*, et al.*, Type 1 diabetic akita mouse hearts are insulin sensitive but manifest structurally abnormal mitochondria that remain coupled despite increased uncoupling protein 3. *Diabetes.* **57,** 2924-2932 (2008).
4. Hsueh W*, et al.*, Recipes for creating animal models of diabetic cardiovascular disease. *Circ Res.* **100,** 1415-1427 (2007).
5. Bugger H*, et al.*, Genetic loss of insulin receptors worsens cardiac efficiency in diabetes. *J Mol Cell Cardiol.* **52,** 1019-1026 (2012).
6. Egom EE*, et al.*, Impaired sinoatrial node function and increased susceptibility to atrial fibrillation in mice lacking natriuretic peptide receptor C. *J Physiol.* **593,** 1127-1146 (2015).
7. Jansen HJ*, et al.*, Atrial structure, function and arrhythmogenesis in aged and frail mice. *Sci Rep.* **7,** 44336 (2017).
8. Azer J, Hua R, Krishnaswamy PS, Rose RA, Effects of natriuretic peptides on electrical conduction in the sinoatrial node and atrial myocardium of the heart. *J Physiol.* **592,** 1025-1045 (2014).
9. Nygren A, Lomax AE, Giles WR, Heterogeneity of action potential durations in isolated mouse left and right atria recorded using voltage-sensitive dye mapping. *Am J Physiol Heart Circ Physiol.* **287,** H2634-2643 (2004).
10. Glukhov AV*, et al.*, Functional anatomy of the murine sinus node: high-resolution optical mapping of ankyrin-B heterozygous mice. *Am J Physiol Heart Circ Physiol.* **299,** H482-491 (2010).
11. Fedorov VV*, et al.*, Application of blebbistatin as an excitation-contraction uncoupler for electrophysiologic study of rat and rabbit hearts. *Heart Rhythm.* **4,** 619-626 (2007).
12. Farman GP*, et al.*, Blebbistatin: use as inhibitor of muscle contraction. *Pflugers Arch.* **455,** 995-1005 (2008).
13. Morley GE*, et al.*, Characterization of conduction in the ventricles of normal and heterozygous Cx43 knockout mice using optical mapping. *J Cardiovasc Electrophysiol.* **10,** 1361-1375 (1999).
14. Springer J*, et al.*, The natriuretic peptides BNP and CNP increase heart rate and electrical conduction by stimulating ionic currents in the sinoatrial node and atrial myocardium following activation of guanylyl cyclase-linked natriuretic peptide receptors. *J Mol Cell Cardiol.* **52,** 1122-1134 (2012).
15. Hua R*, et al.*, Distinct patterns of constitutive phosphodiesterase activity in mouse sinoatrial node and atrial myocardium. *PLoS One.* **7,** e47652 (2012).
16. Lomax AE, Kondo CS, Giles WR, Comparison of time- and voltage-dependent K+ currents in myocytes from left and right atria of adult mice. *Am J Physiol Heart Circ Physiol.* **285,** H1837-1848 (2003).
17. Kuo HC*, et al.*, A defect in the Kv channel-interacting protein 2 (KChIP2) gene leads to a complete loss of I(to) and confers susceptibility to ventricular tachycardia. *Cell.* **107,** 801-813 (2001).
18. Fiset C, Clark RB, Larsen TS, Giles WR, A rapidly activating sustained K+ current modulates repolarization and excitation-contraction coupling in adult mouse ventricle. *J Physiol.* **504 (Pt 3),** 557-563 (1997).

19. Mangoni ME*, et al.*, Functional role of L-type Cav1.3 Ca2+ channels in cardiac pacemaker activity. *Proc Natl Acad Sci U S A.* **100,** 5543-5548 (2003).
20. Zhang Z*, et al.*, Functional roles of Cav1.3(alpha1D) calcium channels in atria: insights gained from gene-targeted null mutant mice. *Circulation.* **112,** 1936-1944 (2005).